Ltr 32.0208

TR-78-450-01
August 1978

CALCULATED AIR QUALITY IMPACT OF THE EMISSIONS FROM THE PROPOSED IPP POWER PLANT AT THE LYNNDYL SITE

Prepared by

J. F. Bowers, H. E. Cramer and A. J. Anderson

Prepared for

INTERMOUNTAIN POWER PROJECT
Post Office Box BB
Sandy, Utah 84070

H. E. Cramer company, inc.

UNIVERSITY OF UTAH RESEARCH PARK
POST OFFICE BOX 8049
SALT LAKE CITY, UTAH 84108

TR-78-450-01
August 1978

CALCULATED AIR QUALITY IMPACT OF THE EMISSIONS FROM THE PROPOSED IPP POWER PLANT AT THE LYNNDYL SITE

Prepared by

J. F. Bowers, H. E. Cramer and A. J. Anderson

Prepared for

INTERMOUNTAIN POWER PROJECT
Post Office Box BB
Sandy, Utah 84070

H. E. Cramer company, inc.

UNIVERSITY OF UTAH RESEARCH PARK
POST OFFICE BOX 8049
SALT LAKE CITY, UTAH 84108

PREFACE

Under Contract No. YA-512-BOA6-8 with the U. S. Department of the Interior, Bureau of Land Management, the H. E. Cramer Company, Inc. evaluated the air quality impact of the proposed Intermountain Power Project (IPP) Power Plant at the primary (Salt Wash) and six alternate sites. The results of the study for BLM are summarized in H. E. Cramer Company, Inc. Technical Report TR-78-311-01 (March 1978). In May 1978, the IPP Board of Directors selected as the prime alternative to the Salt Wash site one of the alternate sites (alternate site A6 or the Lynndyl site) considered in the H. E. Cramer Company's study. On 23 May 1978, the H. E. Cramer Company contracted with IPP to recalculate the air quality impact of the IPP Power Plant at the Lynndyl site, using new plant layout and coal quality data for the site in place of the plant layout and coal quality data for the Salt Wash site used in the original calculations. The results of the new calculations for the Lynndyl site (also known as IPP site L1) are presented in this report. Where appropriate, portions of the March 1978 report to BLM are reproduced in this report with the permission of BLM.

EXECUTIVE SUMMARY

This report describes a diffusion-model analysis of the air quality impact of sulfur dioxide (SO_2), nitrogen dioxide (NO_2) and particulate emissions from the proposed Intermountain Power Project (IPP) plant at the Lynndyl site (IPP site L1). Site L1 is located about 18 kilometers north of Delta, Utah near the center of a broad, flat valley. The proposed IPP Power Plant consists of four 750-megawatt coal-fired generating units for a total capacity of 3,000 megawatts. Emission control equipment will remove approximately 90 percent of the SO_2 and 99.75 percent of the flyash (particulates) from the flue gas. One 216-meter stack will be provided for each pair of units.

The short-term and long-term diffusion models used in the study described in this report were previously developed as part of studies for the U. S. Environmental Protection Agency (EPA) of the air quality impact of SO_2 emissions from sources located in complex terrain. In these previous studies, the short-term and long-term models yielded a good correspondence between concurrent calculated and observed ground-level SO_2 concentrations without recourse to calibration constants that scale calculated concentrations to match observed air quality. Meteorological inputs used in the model calculations were principally developed from hourly surface weather observations made at the Delta, Utah Airport during the period 1949 through 1954. The Delta Airport is located approximately 17 kilometers southeast of site L1. All stack and emissions data used in the study were provided by IPP.

Table I lists the magnitudes and locations of the maximum short-term and annual average ground-level concentrations of SO_2, NO_2 and particulates calculated for the proposed IPP Power Plant at site L1. The National Ambient Air Quality Standards (NAAQS) and the Class I and Class II Non-Deterioration Increments are listed in Table II. The area surrounding site L1 is a Class II (moderate air quality deterioration permitted) region.

TABLE I

MAGNITUDES AND LOCATIONS OF CALCULATED MAXIMUM SHORT-TERM AND ANNUAL AVERAGE SO_2, NO_2 AND PARTICULATE CONCENTRATIONS FOR THE IPP POWER PLANT AT SITE L1

Averaging Time	Concentration ($\mu g/m^3$)			Location	
	SO_2	NO_2	Particulates	Distance (km)	Bearing (deg)
3-Hour	138	-	-	8.0	023
24-Hour	50	-	6	4.0	023
Annual	1.83	8.23*	0.23	6.7	045

*The calculated annual NO_2 concentration assumes that 100-percent of the NO contained in the flue gas is converted to NO_2.

TABLE II

NATIONAL AMBIENT AIR QUALITY STANDARDS
AND NON-DETERIORATION INCREMENTS

Pollutant	Averaging Time	National Ambient Air Quality Standard ($\mu g/m^3$)	Non-Deterioration Increment ($\mu g/m^3$)	
			Class I	Class II
SO_2	3 Hours	1,300	25	512
	24 Hours	365	5	91
	Annual	80	2	20
Particulates	24 Hours	260 (150)*	10	37
	Annual**	75 (60)*	5	19
NO_2	Annual	100	--	--

*The secondary particulate standards are enclosed by parentheses.
**Annual geometric mean.

Comparison of the results of the diffusion-model calculations in Table I with Table II shows that emissions from the proposed IPP Power Plant at site L1 will not endanger any National Ambient Air Quality Standard or Class II Non-Deterioration Increment. The results of the model calculations also show that the only existing or potential Class I (pristine air quality) region likely to be affected by emissions from the IPP plant at site L1 is the Deep Creek Mountains potential Class I region, located 107 kilometers west of site L1. The maximum short-term and annual average SO_2 and particulate concentrations calculated for the Deep Creek Mountains are given in Table III. Comparison of the results of the calculations in Table III with Table II shows that emissions from the proposed IPP Power Plant at site L1 will not endanger the Class I Non-Deterioration Increments at the Deep Creek Mountains.

On the basis of our analysis of topographic, meteorological and air quality data, we believe that significant interactions of emissions from the proposed IPP Power Plant at site L1 with emissions from the pollutant sources along the industrialized Wasatch Front area (Utah, Tooele and Salt Lake Counties) are unlikely because site L1 and the Wasatch Front area are contained in different functional air basins. Also, following the EPA definition of a significant air quality impact, the results of our diffusion-model calculations indicate that the plant will not have a significant impact at the nearest air quality monitoring sites where violations of the National Ambient Air Quality Standards have been measured.

The accuracy of the diffusion models used in this study should be considered in assessing compliance with the National Ambient Air Quality Standards and the Class I and Class II Non-Deterioration Increments. In validation studies for SO_2 sources located in complex terrain, the short-term and long-term diffusion models used in this study have, on the average, calculated SO_2 concentrations within 20 percent of the observed values for all averaging times at distances ranging from about 1 to 30 kilometers from the source. The accuracy of the models has not been established at

TABLE III

MAXIMUM SHORT-TERM AND ANNUAL AVERAGE SO_2 AND PARTICULATE CONCENTRATIONS CALCULATED AT THE DEEP CREEK MOUNTAINS

Averaging Time	Concentration ($\mu g/m^3$)	
	SO_2	Particulates
3 Hour	17.3	--
24 Hour	2.8	0.4
Annual	0.016	0.002

distances greater than about 30 kilometers. Also, the results of the model calculations are biased toward overestimation at longer downwind distances because of the neglect of transport time and the assumed absence of any SO_2 depletion by chemical transformation or surface deposition.

TABLE OF CONTENTS

SECTION 1
INTRODUCTION

1.1 BACKGROUND AND PURPOSE

The Intermountain Power Project (IPP), a consortium of California, Utah and Nevada utilities, originally proposed the construction of a 3,000-megawatt coal-fired electric power generating station at the Salt Wash site in Wayne County, Utah. However, the Federal Land Manager expressed concern about the plant's potential air quality impact at Capitol Reef National Park, 16 kilometers west of the Salt Wash site, and urged the Project to seek an alternate site. During the summer of 1977, the Governor of Utah and the Federal Land Manager formed an Interagency Task Force on Power Plant Siting to assist IPP and others in siting power plants in Utah. After considering a number of factors including air quality impact, the Task Force reported to the Governor of Utah on 8 November 1977 that it considered a site near Lynndyl, Utah to be the best choice as an IPP alternative site.

Under Contract No. YA-512-BOA6-8 with the U. S. Department of the Interior, Bureau of Land Management (BLM), the H. E. Cramer Company, Inc. of Salt Lake City, Utah performed a detailed air quality impact analysis for the proposed IPP Power Plant at the Salt Wash site and six alternate sites. The Task Force's Lynndyl site was included in this analysis as alternate site A6. In a final report to BLM (Bowers, et al., March 1978), the H. E. Cramer Company concluded that "...if air quality impact is the principal consideration, alternate site A6 is clearly the most favorable of the seven sites for the proposed IPP Power Plant considered in this study."

On the basis of the Task Force's recommendation, the conclusions contained in the H. E. Cramer Company's report to BLM and other factors, the IPP Board of Directors selected alternate site A6 (the Lynndyl site,

also known as IPP site L1) as the prime alternative to the Salt Wash site. Because the plant layout and coal quality for the IPP Power Plant at the Lynndyl site differ somewhat from the plant layout and coal quality assumed in the H. E. Cramer Company's original analysis, it is necessary to recalculate the air quality impact in order to satisfy the requirements of the Prevention of Significant Deterioration (PSD) Regulations. Consequently, IPP requested the H. E. Cramer Company to repeat the diffusion-model calculations for the Lynndyl site using the new plant layout and coal quality data. The H. E. Cramer Company formally contracted with IPP on 23 May 1978 to perform the air quality impact calculations for the Lynndyl site.

The purpose of this report is to provide IPP with the results of diffusion-model calculations of the air quality impact of emissions from the proposed IPP Power Plant at the Lynndyl site. Specific calculations described in this report include:

- Maximum annual average ground-level concentrations of sulfur dioxide (SO_2), nitrogen dioxide (NO_2) and particulates
- Maximum 24-hour average ground-level concentrations of SO_2 and particulates
- Maximum 3-hour ground-level SO_2 concentrations

The results of these calculations are presented in the form of ground-level concentration isopleth maps. Additionally, an assessment is made of the plant's air quality impact at the nearest existing and potential Class I regions, and possible interactions of emissions from the plant with emissions from other major pollutant sources are considered.

The above calculations are intended to satisfy the requirements of the PSD Regulations in effect as of 7 August 1978. However, the

H. E. Cramer Company and IPP recognize that the U. S. Environmental Protection Agency (EPA) may promulgate additional requirements after 7 August 1978. Any future requirements will be addressed in supplemental reports.

1.2 DESCRIPTION OF THE SITE

Figure 1-1 is a topographic map of central Utah that shows the location of the Lynndyl site, also identified as IPP site L1. The site is located 18 kilometers north of Delta, Utah at an elevation of 1,420 meters above mean sea level (MSL). The site is near the center of a broad, flat valley which has a north-northeast to south-southwest orientation. The only significant terrain features within a 25-kilometer radius of the site are Fumarole Butte, located 22 kilometers to the northwest, which rises to an elevation 200 meters above plant grade and Sand Mountain, located 21 kilometers to the northeast, which rises to an elevation 700 meters above plant grade.

The nearest existing Class I (pristine air quality) region, Capitol Reef National Park, is over 150 kilometers southeast of site L1. As explained in Section 3.2.2, emissions from the IPP Power Plant at site L1 will not significantly affect the ambient air quality at Capitol Reef or any of the other existing and potential Class I regions in southeastern Utah. To the best of our knowledge, the only region in central Utah that is currently being considered for Class I status is the Deep Creek Mountains area. This region, shown by the hatched area in Figure 1-1, is 107 kilometers west of site L1. On the basis of our previous calculations of the plant's air quality impact at seven sites, we believe that the Deep Creek Mountains area is the only existing or potential Class I region in Utah that might be affected by emissions from the plant at site L1.

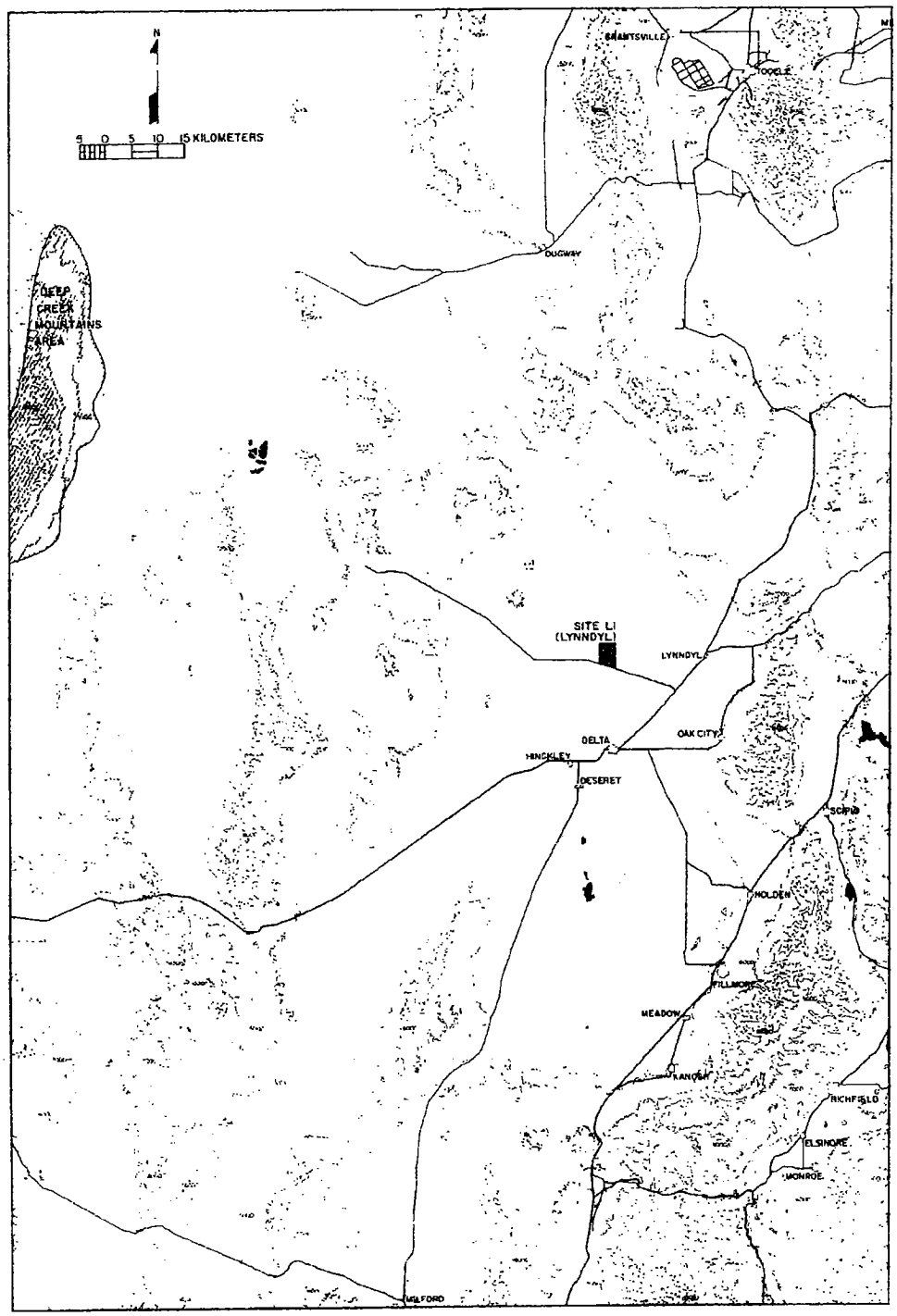

FIGURE 1-1. Topographic map of the area surrounding the Lynndyl site (IPP site L1). Elevations are in feet above mean sea level, and the contour interval is 1,000 feet (305 meters).

1.3 EXISTING AMBIENT AIR QUALITY

Very few ambient air quality data measurements have been made in the vicinity of the Lynndyl site (IPP site L1). Particulate concentration measurements made by the State of Utah during the period August through December 1977 show that the 24-hour secondary National Ambient Air Quality Standard (NAAQS) for particulates of 150 micrograms per cubic meter is exceeded on occasion in nearby Delta, Utah. However, the Utah Bureau of Air Quality believes that the Delta particulate concentration measurements are not representative of the ambient air quality in the Delta area because the hi-vol sampler is located in close proximity to several roads. Consequently, the Bureau of Air Quality plans to relocate the sampler at a representative site where it will not be affected by local fugitive sources.

The major stationary pollutant sources nearest to site L1 are a copper smelter located approximately 140 kilometers to the north-northeast and a steel works located approximately 115 kilometers to the northeast. During periods of north winds, emissions from the smelter are transported along either the east or west side of the Oquirrh Mountains. Emissions that travel to the southwest enter the Rush Valley air basin, which is bounded on the south by the Sheep Rock and Tintic Mountains and on the west by the Stansbury Mountains. Similarly, the steel works is separated from the air basin containing site L1 by the Tintic Mountains. Although there is some interaction at the boundaries of adjacent air basins, we believe that high dilution conditions (moderate-to-strong winds and/or deep surface mixing layers) are required for a significant exchange between air basins to occur. Consequently, we doubt that emissions from the copper smelter, the steel works and the other pollutant sources along the Wasatch Front significantly affect the existing ambient air quality in the vicinity of site L1. We therefore examined the air quality data available for other similar locations in rural Utah in order to estimate the existing ambient air quality at site L1. These air quality data included the data

for the Salt Wash site and Castle Valley, which are discussed in our March 1978 report to BLM, and the data for rural Utah summarized by Berman and Baskett (1976). We excluded from our analysis the data from rural monitoring sites that are near existing stationary pollutant sources (for example, the Huntington Canyon data).

Violations of the 24-hour primary NAAQS for particulates of 260 micrograms per cubic meter and/or the 24-hour secondary NAAQS for particulates of 150 micrograms per cubic meter are found to occur on occasion at all minitoring sites in rural Utah at which particulate concentration measurements are routinely made. The only location at which a violation of the 24-hour secondary standard was not observed is the Salt Wash site. However, measurements at the Salt Wash site were limited to 2- to 3-week periods in each season. The high short-term particulate concentrations found in rural Utah appear to be caused by the natural background and activities such as agriculture, cattle grazing and transportation. For example, Hill, et al. (1976) analyzed filter samples for days with the highest observed particulate concentrations in the Castle Valley and found wind-blown soil dust to be the primary constituent. The occasional high short-term particulate concentrations in rural Utah do not endanger the primary annual (geometric mean) NAAQS of 75 micrograms per cubic meter or the secondary annual (geometric mean) NAAQS of 60 micrograms per cubic meter. Although observed annual geometric mean particulate concentrations in rural Utah are typically on the order of 20 micrograms per cubic meter, measurements in rural Idaho (Record, et al., 1975) indicate that annual geometric mean concentrations of 35 to 45 micrograms per cubic meter are possible in the rural Intermountain Area.

Hourly SO_2 concentrations at most locations in rural Utah are almost always below the monitor threshold of 26 micrograms per cubic meter. For comparison, the annual NAAQS for SO_2 is 80 micrograms per cubic meter. The highest 3-hour and 24-hour average SO_2 concentrations reported by Berman and Baskett (1976) for rural Utah are 156 and 60 micrograms per

cubic meter, respectively. Both concentrations, which were measured in the Warner Valley in southern Utah, are well below the 3-hour and 24-hour NAAQS for SO_2 of 1,300 and 365 micrograms per cubic meter, respectively. The Warner Valley SO_2 concentrations are relatively high in comparison with the SO_2 concentrations observed at other locations in rural Utah.

To the best of our knowledge, no 24-hour average NO_2 concentration in excess of the annual NAAQS for NO_2 of 100 micrograms per cubic meter has been measured in rural Utah. Typical maximum 24-hour average NO_2 concentrations in rural Utah are 25 to 30 micrograms per cubic meter, although somewhat higher values have been measured in the Warner Valley.

Very few ozone (O_3) concentration measurements have been made in rural Utah. The highest measured hourly O_3 concentration contained in the data we examined for rural Utah is 132 micrograms per cubic meter at the Salt Wash site. This concentration is about 83 percent of the existing 1-hour NAAQS for O_3 of 160 micrograms per cubic meter and 66 percent of the proposed NAAQS of 200 micrograms per cubic meter. Ozone concentrations of this magnitude have been measured in remote areas as a result of thunderstorms or stratospheric injections associated with storm systems. Long-range transport of smog from large urban areas has also been hypothesized as a potential cause of high short-term O_3 concentrations in rural areas.

In summary, Table 1-1 gives the NAAQS and the ranges of maximum pollutant concentrations estimated for site L1 on the basis of the air quality data available for rural Utah. As shown by the table, the existing ambient air quality in rural Utah is generally very good. The data indicate that the only ambient air quality standards that may be exceeded at site L1 are the 24-hour primary and secondary NAAQS for particulates. However, analyses of filter samples indicate that wind-blown soil dust

TABLE 1-1

NATIONAL AMBIENT AIR QUALITY STANDARDS AND ESTIMATED EXISTING AMBIENT AIR QUALITY IN THE AREA SURROUNDING SITE L1

Pollutant	Averaging Time	National Ambient Air Quality Standard ($\mu g/m^3$)	Estimated Maximum Concentration ($\mu g/m^3$)
SO_2	3-Hour	1,300	< 13 - 156
	24-Hour	365	< 13 - 60
	Annual	80	< 13
Particulates	24-Hour	260 (150)*	90 - 364
	Annual**	75 (60)*	19 - 45
NO_2	Annual	100	13
O_3	1-Hour	160 - Existing 200 - Proposed	132

*The secondary particulate standards are enclosed by parentheses.

**Annual geometric mean.

is primarily responsible for the occasional high short-term particulate concentrations in rural Utah. According to the current Prevention of Significant Deterioration (PSD) Regulations (Federal Register, Vol. 43, No. 118, p. 26398), infrequent violations of the short-term NAAQS for particulates in a rural area should not prevent the construction of a new stationary source if the source has the requisite degree of particulate emission control.

1.4 REPORT ORGANIZATION

In addition to the Introduction, this report consists of three major sections and two appendices. The source and meteorological data used in the diffusion-model calculations are given in Section 2. The calculation procedures and the results of the calculations are discussed in Section 3. Section 4 summarizes the results of our analysis and identifies the major areas of uncertainty in the diffusion-model calculations. The diffusion models used in this study are described in detail in Appendix A. The hourly meteorological inputs used in the short-term concentration calculations are listed in Appendix B.

SECTION 2
SOURCE AND METEOROLOGICAL DATA

2.1 SOURCE INPUT PARAMETERS

The proposed IPP Power Plant consists of four 750-megawatt generating units. A lime-slurry-spray flue gas desulfurization (FGD) system will remove about 90 percent of the SO_2 from the flue gas. Additionally, electrostatic precipitators in combination with the FGD system will remove 99.75 percent of the flyash (particulates) from the flue gas. One 216-meter stack will be provided for each pair of units. Each stack will have two inner flues with diameters of 9.1 meters, leading to an effective stack diameter of 12.9 meters. An advantage of this design is that the stack exit velocity is not decreased when only one unit is in operation. Thus, the possibility that downwash in the lee of the stack will affect buoyant plume rise during periods of strong winds is reduced.

Stack and emissions parameters for the proposed IPP Power Plant were provided to us by Mr. James H. Anthony, IPP Project Engineer, and were submitted to BLM, EPA Region VIII and the Utah Bureau of Air Quality for review prior to use in this study. We checked the emissions parameters provided by IPP for internal consistency but did not make any independent calculations in order to confirm their validity.

The coal for the IPP Power Plant at the Lynndyl site (IPP site L1) probably will be obtained from existing mines and/or leases in the area considered in the Central Utah Regional Coal Impact Statement. According to IPP, the average coal characteristics over the life of the plant are expected to be 12,000 British Thermal Units (BTU) per pound, a sulfur content of 0.61 percent and an ash content of 8.8 percent. However, the worst-case emission rates used in this study were obtained by modifying the average coal quality. The heat (BTU) content was reduced by 15 percent, the sulfur content was increased by 30 percent

and the ash content was increased by 15 percent. The resulting coal characteristics are 10,200 BTU per pound, a sulfur content of 0.79 percent and an ash content of 10.1 percent.

The physical stack parameters and worst-case emissions data for the proposed IPP Power Plant at site L1 are given in Table 2-1. Table 2-1 includes the Universal Transverse Mercator (UTM) coordinates of the stacks and the elevations of the stack bases above mean sea level (MSL). The new stack locations are approximately 3.4 kilometers east-southeast of the locations assumed in our previous calculations for alternate site A6. The stack height of 216 meters corresponds to the definition of "good engineering practice" in stack design given in the 1977 Clean Air Act Amendments. That is, the stack height is 2.5 times the height of the tallest plant structure. According to IPP, the proposed power plant will operate at full load except for down time, which is expected to reduce plant generation on an annual basis to about 85 percent of the maximum possible generation. Consequently, the parameters in Table 2-1 that are used to calculate plume rise have values that correspond to full-load operation, while the annual average pollutant emission rates are the worst-case emission rates, reduced to 85 percent of the full-load emission rates. It should be noted that the NO_2 emission rates assume that 100 percent of the NO molecules in the plumes are converted to NO_2. However, measurements in the plumes from coal-fired power plants in the western United States indicate that only about 10 percent of the NO_x (NO plus NO_2) molecules are initially in the form of NO_2 (for example, see Ogren, et al., 1977).

TABLE 2-1

STACK PARAMETERS AND WORST-CASE EMISSIONS DATA
FOR THE IPP POWER PLANT AT SITE L1

Parameter	Parameter Value	
	Stack No. 1	Stack No. 2
Stack Height (m)	216	216
Stack Inner Diameter* (m)	12.9	12.9
UTM X Coordinate (m)	363,450	363,650
UTM Y Coordinate (m)	4,374,270	4,374,270
Stack Base Elevation (m above MSL)	1,420	1,420
Volumetric Emission Rate (m^3/sec)	2,718	2,718
Stack Exit Temperature (^oK)	350	350
Stack Exit Velocity (m/sec)	21	21
SO_2 Emission Rate (g/sec)		
Maximum Short-Term	292.4	292.4
Annual Average	248.5	248.5
Particulate Emission Rate**(g/sec)		
Maximum Short-Term	37.4	37.4
Annual Average	31.8	31.8
Annual Average NO_2 Emission Rate***(g/sec)	1,123.7	1,123.7

*Effective diameter for two inner flues with diameters of 9.1 meters
**The particulate emission rates assume that 20 percent of the flyash is contained in the bottom ash and 80 percent is contained in the flue gas.
***The NO_2 emission rate assumes 100-percent conversion of NO to NO_2.

2.2 METEOROLOGICAL DATA

2.2.1 Selection of Representative Wind Data

The Lynndyl site (IPP site L1) is located near the center of a broad valley approximately 17 kilometers northwest of the Delta, Utah Airport (see Figure 1-1). No elevated terrain features exist between site L1 and the Delta Airport. We obtained from the National Climatic Center a computer tape containing hourly surface weather observations made at the Delta Airport during the 6-year period from January 1949 through December 1954. Figure 2-1 shows the annual wind-direction distribution at the Delta Airport during this period. The directions in Figure 2-1 are reversed 180 degrees and are the directions toward which the wind is blowing. Reversed wind directions are used in Figure 2-1 because the annual distribution of pollutants emitted from a single source closely resembles the reversed annual wind-direction distribution. In general, the most frequent wind directions reflect the approximate north-northeast to south-southwest orientation of the valley. Local influences (for example, light nighttime drainage winds from the elevated terrain east of the Delta Airport) are most likely to control the low-level winds during periods of light winds. However, the most frequent wind directions for light wind speeds at the Delta Airport are also the most frequent wind directions for moderate-to-strong wind speeds. Thus, the Delta wind data do not show any significant local influences that would make the data non-representative of conditions at site L1. We therefore conclude that the meteorological data from the Delta Airport are suitable for use in diffusion-model calculations at site L1.

2.2.2 Meteorological Inputs for the Annual Concentration Calculations

We used the hourly surface weather observations made at the Delta Airport during the period 1949 through 1954 to generate seasonal and annual distributions of wind-speed and wind-direction categories,

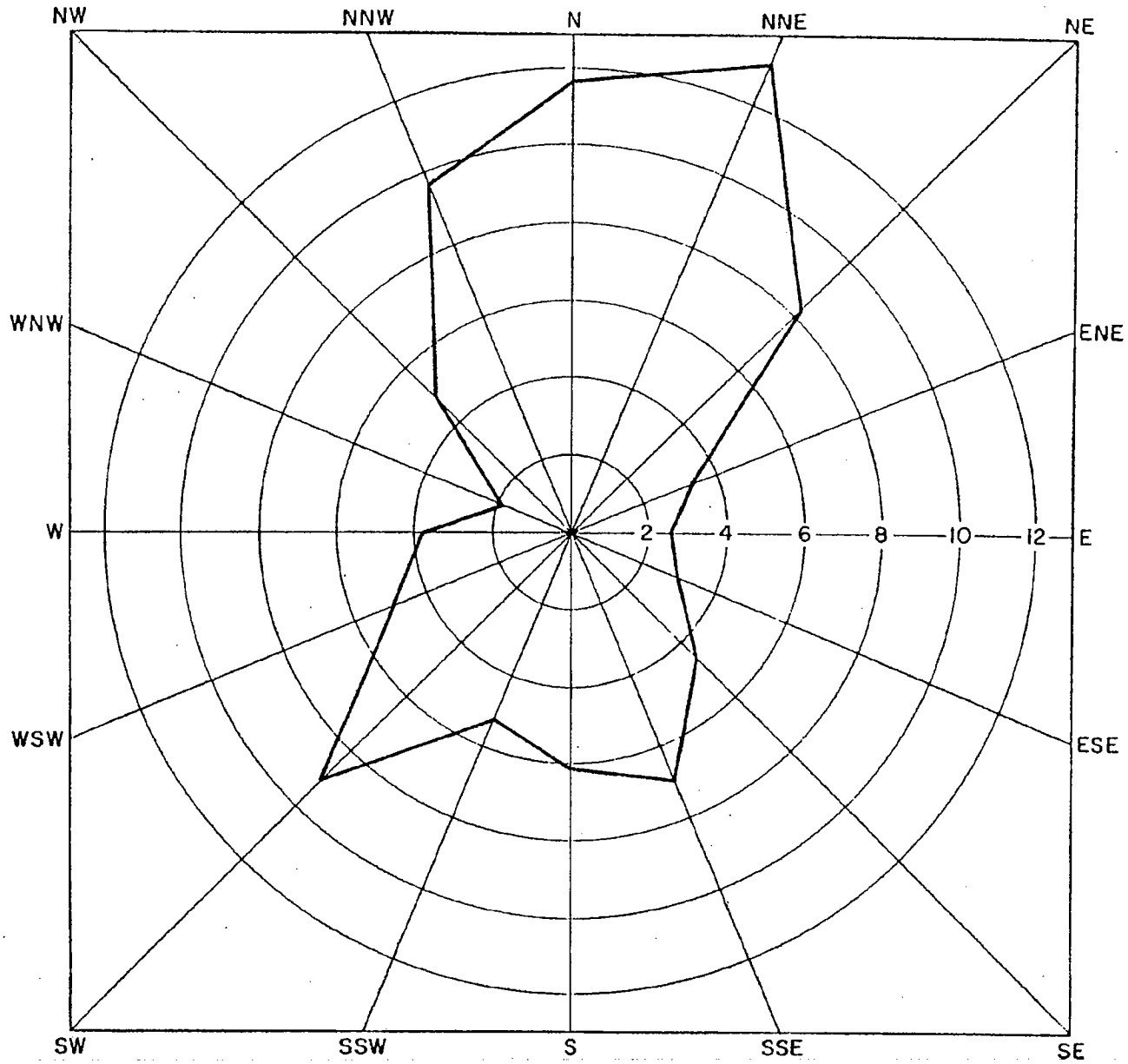

FIGURE 2-1. Annual wind-direction distribution at Delta, Utah during the period 1949-1954. Directions are directions toward which the wind is blowing, and the frequency scale is shown at the right center of the figure.

classified according to the Pasquill stability categories. These distributions were developed using the Turner (1964) definitions of the Pasquill stability cateogires, which are based on solar radiation (insolation) and wind speed. Tables 2-2 and 2-3 list the parameters that define the various stability categories. The thermal stratifications represented by the Pasquill stability categories are:

- A - Very unstable
- B - Unstable
- C - Slight unstable
- D - Neutral
- E - Stable
- F - Very stable

The annual wind summary for the Delta Airport is given in Table 2-4.

As explained in Appendix A, our models use a wind-profile exponent law to adjust the mean wind speed from the measurement height to the stack height for the plume rise calculations and to the plume stabilization height for the concentration calculations. Table 2-5 lists the wind-profile exponents used in the calculations for the various combinations of wind-speed and stability categories. These exponents are principally based on the results obtained by Cramer, et al. (1972) for Dugway Proving Ground, Utah and are consistent with the results obtained by DeMarrais (1959) at Brookhaven National Laboratory. The wind-profile exponents recently developed for a number of locations by Touma (1977) also support the use of the wind-profile exponents given in Table 2-5.

The equation for the standard deviation of the lateral concentration distribution σ_y in our short-term diffusion model includes the effects of entrainment on initial plume growth and relates σ_y directly to the lateral turbulent intensity or standard deviation of the wind azimuth angle σ_A' (see Equation (A-11) in Appendix A). Similarly, the

TABLE 2-2

PASQUILL STABILITY CATEOGRY AS A
FUNCTION OF ISOLATION
AND WIND SPEED

Wind Speed (Knots)	Insolation Index						
	4	3	2	1	0	-1	-2
0,1	A	A	B	C	D	F	F
2,3	A	B	B	C	D	F	F
4,5	A	B	C	D	D	E	F
6	B	B	C	D	D	E	F
7	B	B	C	D	D	D	E
8,9	B	C	C	D	D	D	E
10	C	C	D	D	D	D	E
11	C	C	D	D	D	D	D
≥12	C	D	D	D	D	D	D

TABLE 2-3

INSOLATION CATEGORIES

Insolation	Insolation Category Number
Strong	4
Moderate	3
Slight	2
Weak	1
Overcast < 7,000 feet (day or night)	0
Cloud Cover > 4/10 (night)	-1
Cloud Cover ≤ 4/10 (night)	-2

TABLE 2-4

ANNUAL JOINT FREQUENCY OF OCCURRENCE OF WIND SPEED AND WIND DIRECTION AT THE DELTA, UTAH AIRPORT

DIRECTION (SECTOR)	STABILITY CATEGORY A WIND SPEED (M/SEC) 0-1.5	1.6-3.0	TOTAL	STABILITY CATEGORY B WIND SPEED (M/SEC) 0-1.5	1.6-3.0	3.1-5.1	TOTAL	STABILITY CATEGORY C WIND SPEED (M/SEC) 0-1.5	1.6-3.0	3.1-5.1	5.2-8.2	8.3-10.8	>10.8	TOTAL
N	.0013	.0002	.0015	.0044	.0011	.0006	.0061	.0020	.0017	.0025	.0001	.0001	.0000	.0064
NNE	.0010	.0002	.0013	.0032	.0010	.0004	.0046	.0012	.0013	.0017	.0001	.0000	.0000	.0042
NE	.0011	.0001	.0012	.0053	.0005	.0001	.0059	.0026	.0012	.0011	.0000	.0000	.0000	.0050
ENE	.0004	.0001	.0004	.0025	.0003	.0001	.0030	.0017	.0008	.0006	.0000	.0000	.0000	.0031
E	.0005	.0001	.0006	.0026	.0002	.0001	.0029	.0015	.0007	.0002	.0000	.0000	.0000	.0024
ESE	.0004	.0001	.0005	.0013	.0002	.0000	.0015	.0006	.0003	.0002	.0000	.0000	.0000	.0011
SE	.0006	.0000	.0007	.0039	.0007	.0001	.0047	.0018	.0008	.0009	.0001	.0000	.0000	.0036
SSE	.0009	.0001	.0010	.0047	.0008	.0005	.0060	.0020	.0016	.0022	.0001	.0000	.0000	.0059
S	.0013	.0002	.0016	.0073	.0014	.0009	.0096	.0034	.0025	.0049	.0004	.0003	.0001	.0116
SSW	.0020	.0006	.0026	.0091	.0029	.0021	.0141	.0029	.0035	.0090	.0010	.0010	.0010	.0184
SW	.0041	.0009	.0050	.0105	.0037	.0030	.0173	.0037	.0030	.0071	.0010	.0007	.0006	.0161
WSW	.0026	.0008	.0035	.0053	.0026	.0020	.0099	.0012	.0016	.0042	.0006	.0002	.0001	.0079
W	.0020	.0006	.0026	.0046	.0017	.0012	.0074	.0015	.0012	.0020	.0001	.0000	.0000	.0048
WNW	.0019	.0006	.0024	.0056	.0022	.0013	.0091	.0013	.0015	.0025	.0001	.0000	.0000	.0054
NW	.0017	.0003	.0020	.0053	.0019	.0009	.0080	.0015	.0015	.0029	.0001	.0000	.0000	.0059
NNW	.0011	.0004	.0015	.0056	.0019	.0012	.0088	.0018	.0018	.0048	.0003	.0002	.0001	.0089
TOTAL	.0229	.0053	.0282	.0812	.0231	.0144	.1188	.0307	.0249	.0467	.0040	.0026	.0019	.1107

DIRECTION (SECTOR)	STABILITY CATEGORY D WIND SPEED (M/SEC) 0-1.5	1.6-3.0	3.1-5.1	5.2-8.2	8.3-10.8	>10.8	TOTAL	STABILITY CATEGORY E WIND SPEED (M/SEC) 1.6-3.0	3.1-5.1	TOTAL	STABILITY CATEGORY F WIND SPEED (M/SEC) 0-1.5	1.6-3.0	TOTAL	ANNUAL WIND DIRECTION DISTRIBUTION
N	.0018	.0020	.0065	.0056	.0021	.0006	.0208	.0026	.0064	.0090	.0122	.0057	.0179	.0617
NNE	.0015	.0013	.0064	.0036	.0010	.0003	.0141	.0026	.0074	.0100	.0127	.0072	.0199	.0541
NE	.0025	.0020	.0056	.0022	.0004	.0001	.0130	.0048	.0117	.0166	.0337	.0165	.0502	.0918
ENE	.0012	.0016	.0027	.0008	.0002	.0000	.0065	.0035	.0048	.0083	.0180	.0105	.0285	.0498
E	.0015	.0011	.0020	.0002	.0000	.0000	.0048	.0028	.0018	.0046	.0175	.0062	.0237	.0390
ESE	.0006	.0006	.0014	.0006	.0001	.0000	.0035	.0014	.0017	.0032	.0069	.0026	.0096	.0193
SE	.0019	.0015	.0070	.0028	.0005	.0001	.0138	.0025	.0067	.0092	.0135	.0052	.0187	.0507
SSE	.0021	.0024	.0202	.0123	.0028	.0007	.0407	.0041	.0169	.0210	.0156	.0074	.0230	.0975
S	.0034	.0030	.0200	.0165	.0076	.0031	.0536	.0043	.0136	.0179	.0160	.0075	.0235	.1178
SSW	.0027	.0038	.0154	.0197	.0168	.0144	.0728	.0031	.0054	.0085	.0112	.0052	.0164	.1327
SW	.0026	.0025	.0077	.0078	.0050	.0045	.0281	.0022	.0020	.0042	.0094	.0027	.0120	.0826
WSW	.0014	.0014	.0045	.0025	.0016	.0005	.0098	.0008	.0004	.0012	.0029	.0008	.0037	.0361
W	.0015	.0010	.0013	.0007	.0002	.0000	.0047	.0004	.0004	.0008	.0033	.0008	.0041	.0244
WNW	.0013	.0010	.0023	.0013	.0004	.0002	.0064	.0007	.0005	.0012	.0038	.0013	.0051	.0297
NW	.0023	.0016	.0056	.0039	.0022	.0004	.0156	.0012	.0019	.0031	.0062	.0021	.0082	.0429
NNW	.0020	.0024	.0113	.0105	.0049	.0021	.0332	.0019	.0042	.0061	.0074	.0043	.0117	.0701
TOTAL	.0304	.0292	.1177	.0915	.0458	.0269	.3413	.0389	.0859	.1248	.1903	.0860	.2763	

TABLE 2-5

WIND-PROFILE EXPONENTS USED IN THE CONCENTRATION CALCULATIONS FOR SITE L1

Pasquill Stability Category	Wind Speed (m/sec)					
	0.0-1.5	1.6-3.0	3.1-5.1	5.2-8.2	8.3-10.8	>10.8
A	0.10	0.10	--	--	--	--
B	0.10	0.10	0.10	--	--	--
C	0.20	0.15	0.10	0.10	0.10	0.10
D	0.25	0.20	0.15	0.10	0.10	0.10
E	--	0.25	0.20	--	--	--
F	0.40	0.30	--	--	--	--

TABLE 2-6

HOURLY VERTICAL AND LATERAL TURBULENT INTENSITIES USED IN THE CONCENTRATION CALCULATIONS FOR SITE L1

Pasquill Stability Category	σ'_E (rad)	σ'_A (rad)
A	0.1745	0.2495
B	0.1080	0.1544
C	0.0735	0.1051
D	0.0465	0.0665
E	0.0350	0.0501
F	0.0235	0.0336

equation for the standard deviation of the vertical concentration distribution σ_z in our short-term and long-term diffusion models also includes the effects of entrainment on initial plume growth and relates σ_z directly to the vertical turbulent intensity or standard deviation of the wind elevation angle σ_E' (see Equation (A-13) in Appendix A). Table 2-6 lists the hourly vertical and lateral turbulent intensities used in the concentration calculations for site L1. The vertical turbulent intensities σ_E' are based in part on the measurements of Luna and Church (1971) and are consistent with the σ_E' values implicit in the vertical expansion curves presented by Pasquill (1961). In accord with the measurements of Luna and Church (1971) and others, we assume that σ_A' and σ_E' are approximately equivalent for a 10-minute averaging time at heights above the surface of 100 meters or more. We also assume that σ_E' is approximately constant for averaging times ranging from 10 to 60 minutes, while σ_A' increases according to a $t^{1/5}$ law (Osipov, 1972 and others).

The locations nearest site L1 for which detailed mixing-depth statistics are available are Salt Lake City, Utah (Environmental Data Service, 1968) and Grand Junction, Colorado (Environmental Data Service, 1966). As part of our previous study for BLM, we analyzed the mixing depth data for these locations and found that the median early morning mixing depths at Grand Junction and Salt Lake City are essentially the same, but the afternoon median mixing depths at Grand Junction are consistently larger than the corresponding mixing depths at Salt Lake City. As shown by Figures 3-28 through 3-31 of Cramer, et al. (1972), the seasonal early morning mixing depths at Salt Lake City are in good agreement with the median nighttime mixing depths at Dugway Proving Ground, which is located 75 kilometers north of site L1. Although afternoon mixing depth measurements at Dugway Proving Ground are only made in support of mission requirements, our experience in analyzing data collected during field diffusion experiments at Dugway Proving Ground indicates that there is a good correspondence between the

mixing depths at Salt Lake City and Dugway Proving Ground. Additionally, the isopleths of mean early morning and afternoon mixing depths given by Holzworth (1972) suggest that the Salt Lake City mixing depths are likely to be representative of mixing depths at site L1. We therefore selected the Salt Lake City median mixing depths given in Table 2-7 for use in the concentration calculations at site L1. The seasonal median afternoon mixing depths at Salt Lake City were assigned to the unstable A, B and C stability categories; the seasonal median early morning mixing depths were assigned to the stable E and F stability categories; and the seasonal median early morning and afternoon mixing depths were averaged and assigned to the neutral D stability category.

The plume rise equations given in Section A.2 of Appendix A require the vertical potential temperature gradient and ambient air temperature as inputs. The vertical potential temperature gradients and ambient air temperatures used in the annual concentration calculations at site L1 are given in Tables 2-8 and 2-9, respectively. The potential temperature gradients in Table 2-8 are based on the measurements of Luna and Church (1971), the Pasquill (1961) and Turner (1964) definitions of the Pasquill stability categories, and our previous experience. The ambient air temperatures in Table 2-9 are based on hourly temperature measurements made at the Delta Airport during the period 1949 through 1954. The seasonal average afternoon temperatures were assigned to the unstable A, B and C stability categories; the seasonal average nighttime temperatures were assigned to the stable E and F stability categories; and the seasonal average temperatures for the morning and evening periods were assigned to the neutral D stability category. The hours that comprise the seasonal time-of-day categories are listed in Table 2-10.

2.2.3 Meteorological Inputs for the Short-Term Concentration Calculations

The hourly meteorological inputs used in the "worst-case" 3-hour and 24-hour average concentration calculations for site L1 are

TABLE 2-7

SEASONAL MEDIAN MIXING DEPTHS IN METERS
BASED ON SALT LAKE CITY DATA

Pasquill Stability Category	Wind Speed (m/sec)					
	0.0-1.5	1.6-3.0	3.1-5.1	5.2-8.2	8.3-10.8	>10.8
(a) Winter						
A	400	550	--	--	--	--
B	400	550	800	--	--	--
C	400	550	800	1,000	1,000	1,000
D	265	340	460	675	675	840
E	--	125	125	--	--	--
F	125	125	--	--	--	--
(b) Spring						
A	2,000	2,250	--	--	--	--
B	2,000	2,250	2,500	--	--	--
C	2,000	2,250	2,500	2,500	2,500	2,500
D	1,060	1,190	1,310	1,350	1,425	1,950
E	--	125	125	--	--	--
F	125	125	--	--	--	--
(c) Summer						
A	2,500	2,900	--	--	--	--
B	2,500	2,900	3,500	--	--	--
C	2,500	2,900	3,500	3,700	4,000	4,000
D	1,310	1,510	1,810	1,950	2,250	2,400
E	--	125	125	--	--	--
F	125	125	--	--	--	--
(d) Fall						
A	800	1,250	--	--	--	--
B	800	1,250	1,600	--	--	--
C	800	1,250	1,600	2,000	2,250	2,500
D	460	690	860	1,125	1,275	1,625
E	--	125	125	--	--	--
F	125	125	--	--	--	--

TABLE 2-8

VERTICAL POTENTIAL TEMPERATURE GRADIENTS IN DEGREES KELVIN PER METER USED IN THE CONCENTRATION CALCULATIONS FOR SITE L1

Pasquill Stability Category	Wind Speed (m/sec)					
	0.0-1.5	1.6-3.0	3.1-5.1	5.2-8.2	8.3-10.8	>10.8
A	0.000	0.000	--	--	--	--
B	0.000	0.000	0.000	--	--	--
C	0.000	0.000	0.000	0.000	0.000	0.000
D	0.020	0.010	0.005	0.000	0.000	0.000
E	--	0.020	0.010	--	--	--
F	0.040	0.030	--	--	--	--

TABLE 2-9

AMBIENT AIR TEMPERATURES IN DEGREES KELVIN USED IN THE CONCENTRATION CALCULATIONS FOR SITE L1

Pasquill Stability Category	Season			
	Winter	Spring	Summer	Fall
A	276	289	302	292
B	276	289	302	292
C	276	289	302	292
D	272	284	296	286
E	268	279	290	280
F	268	279	290	280

TABLE 2-10

SEASONAL TIME-OF-DAY
CATEGORIES

Season	Time (MST)			
	Night	Morning	Afternoon	Evening
Winter	1900 - 0800	0800 - 1200	1200 - 1600	1600 - 1900
Spring	2000 - 0700	0700 - 1100	1100 - 1700	1700 - 2000
Summer	2200 - 0600	0600 - 1000	1000 - 1900	1900 - 2200
Fall	2000 - 0700	0700 - 1100	1100 - 1700	1700 - 2000

contained in Appendix B. The selection of these "worst-case" periods is discussed in Section 3.2.1. The "worst-case" 3-hour period for the Deep Creek Mountains potential Class I region (see Figure 1-1) was selected as follows:

1. The 1949-1954 Delta Airport wind data were analyzed to isolate all periods when wind speeds greater than 1.5 meters per second persisted for 3 or more hours within any standard 22.5-degree wind-direction sector that would permit emissions from the IPP Power Plant located at site L1 to be transported toward the Deep Creek Mountains.

2. Periods when the IPP plumes would have stabilized above the top of the surface mixing layer and thus would not have mixed to the surface were deleted from the candidate list of "worst-case" 3-hour periods. The mixing depths were estimated from Table 2-7.

3. The reduced list was further reduced to the ten periods with the poorest dilution conditions at long downwind distances (i.e., shallow mixing depths, light wind speeds and the most stable Pasquill stability categories consistent with the plumes being contained within the surface mixing layer.

4. The periods selected in Step 3 were again reduced to the five periods with wind directions that minimized the travel distance between site L1 and the Deep Creek Mountains. Concentrations were calculated for all of these periods.

Similar procedures were used to select the "worst-case" 24-hour periods for the Deep Creek Mountains except that the number of hours of the persistence of wind direction within the sector or sectors required to transport emissions toward the Deep Creek Mountains was usually the first consideration.

To the maximum extent possible, observed meteorological data were used in the short-term concentration calculations for site L1. The Delta Airport wind directions, which were reported to the nearest 22.5-degree sector, were used directly in the "worst-case" 3-hour and 24-hour concentration calculations for any point (i.e., in the vicinity of the plant). In the case of the Deep Creek Mountains, the hourly wind direction was set equal to the direction within the standard wind-direction sector that minimized the travel distance to the Deep Creek Mountains. The Delta Airport wind speeds and ambient air temperatures were also used as model inputs. The vertical potential temperature gradients and wind-profile exponents were assigned to each hour on the basis of stability and wind speed (see Tables 2-5 and 2-8); mixing depths were assigned on the basis of season, stability and wind speed (see Table 2-7); and the lateral and vertical turbulent intensities were assigned on the basis of stability (see Table 2-6). Because the Delta Airport wind directions were reported to the nearest 22.5-degree sector, an N-hour lateral turbulent intensity (obtained using the $t^{1/5}$ law of Osipov, 1972 and others) was assigned to each hour of an N-hour period with the same wind direction and stability in order to account in part for the effects of the actual variability of the wind direction. The EPA CRSTER Model modifies the reported wind directions by means of a random number generator in a similar attempt to account for these effects. We point out that, in our opinion, the use of wind directions reported to the nearest 22.5-degree sector in combination with N-hour turbulent intensities probably biased the short-term concentrations calculated for site L1 toward overestimation.

SECTION 3
CALCULATION PROCEDURES AND RESULTS

3.1 ANNUAL AVERAGE GROUND-LEVEL CONCENTRATIONS

The source data in Section 2.1 and the meteorological inputs discussed in Section 2.2 were used with the long-term concentration model described in Section A.4 of Appendix A to calculate seasonal and annual average ground-level SO_2, NO_2, and particulate concentrations for the proposed IPP Power Plant located at the Lynndyl site (IPP site L1). The calculation grid consisted of 1,681 points spaced at 1-kilometer intervals on a 40-kilometer by 40-kilometer grid approximately centered on the plant site. Additional grid points were placed along the boundaries of the Deep Creek Mountains potential Class I region, the only existing or potential Class I region likely to be affected by emissions from site L1 (see Section 3.2.2). The procedures described in Section A.5 of Appendix A were used to account for the effects of variations in terrain height over the calculation grid.

The calculated isopleths of annual average ground-level concentrations of SO_2, NO_2 and particulates are shown in Figures 3-1, 3-2 and 3-3, respectively. The magnitudes and location of the calculated maximum annual concentrations are given in Table 3-1. The annual Class II Non-Deterioration Increments for SO_2 and particulates are 20 and 19 micrograms per cubic meter, respectively. The calculated maximum annual SO_2 concentration of 1.83 micrograms per cubic meter is about 9.2 percent of the Class II Increment for SO_2 and the calculated maximum annual particulate concentration of 0.23 micrograms per cubic meter is about 1.2 percent of the Class II Increment for particulates. Similarly, the calculated maximum NO_2 concentration of 8.23 micrograms per cubic meter is about 8.2 percent of the annual National Ambient Air Quality Standard (NAAQS) for NO_2 of 100 micrograms per cubic meter (at present, there are no Non-deterioration Increments for NO_2). As noted in Section

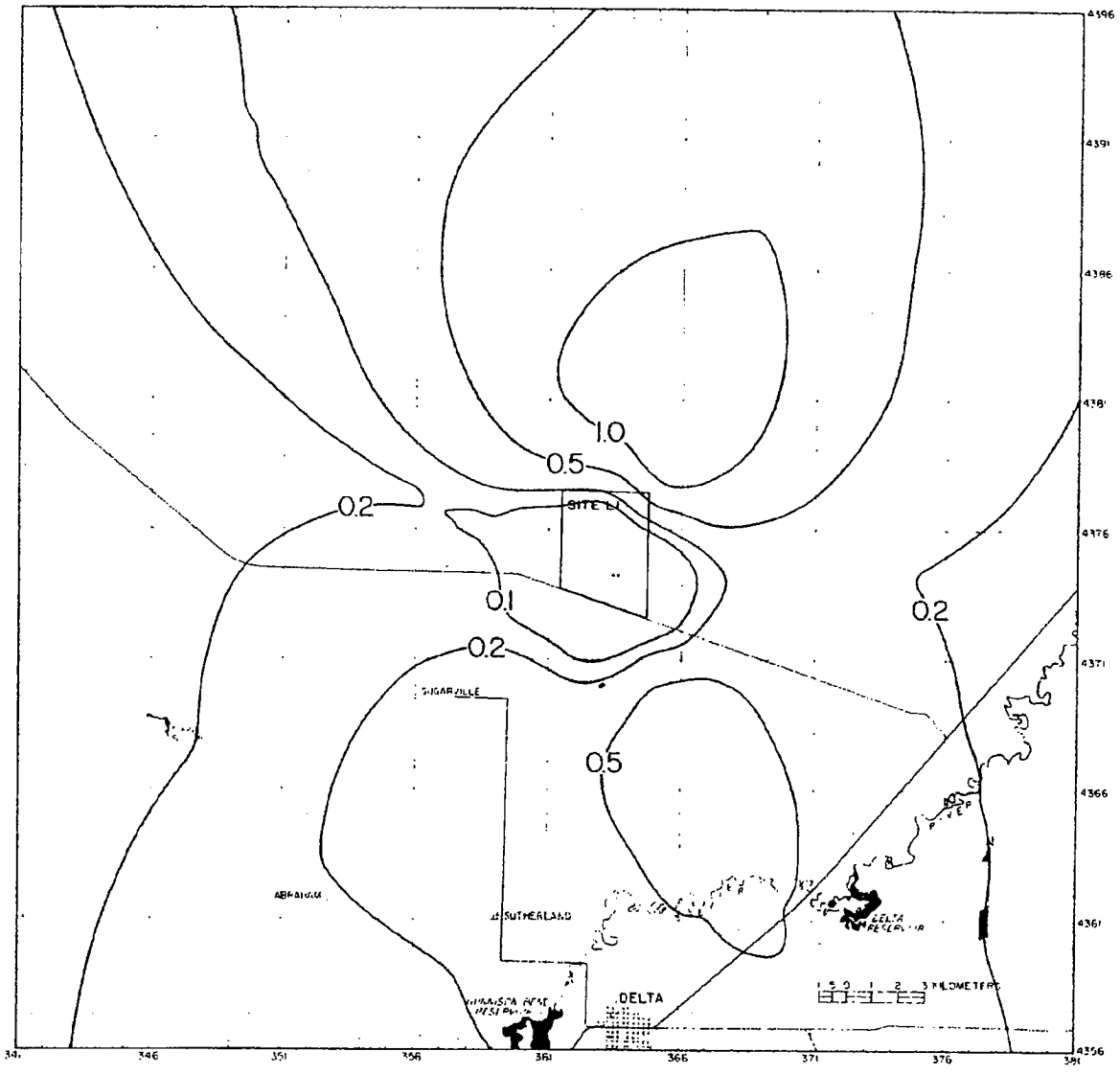

FIGURE 3-1. Calculated isopleths of annual average ground-level SO_2 concentration in micrograms per cubic meter for the IPP Power Plant located at site L1.

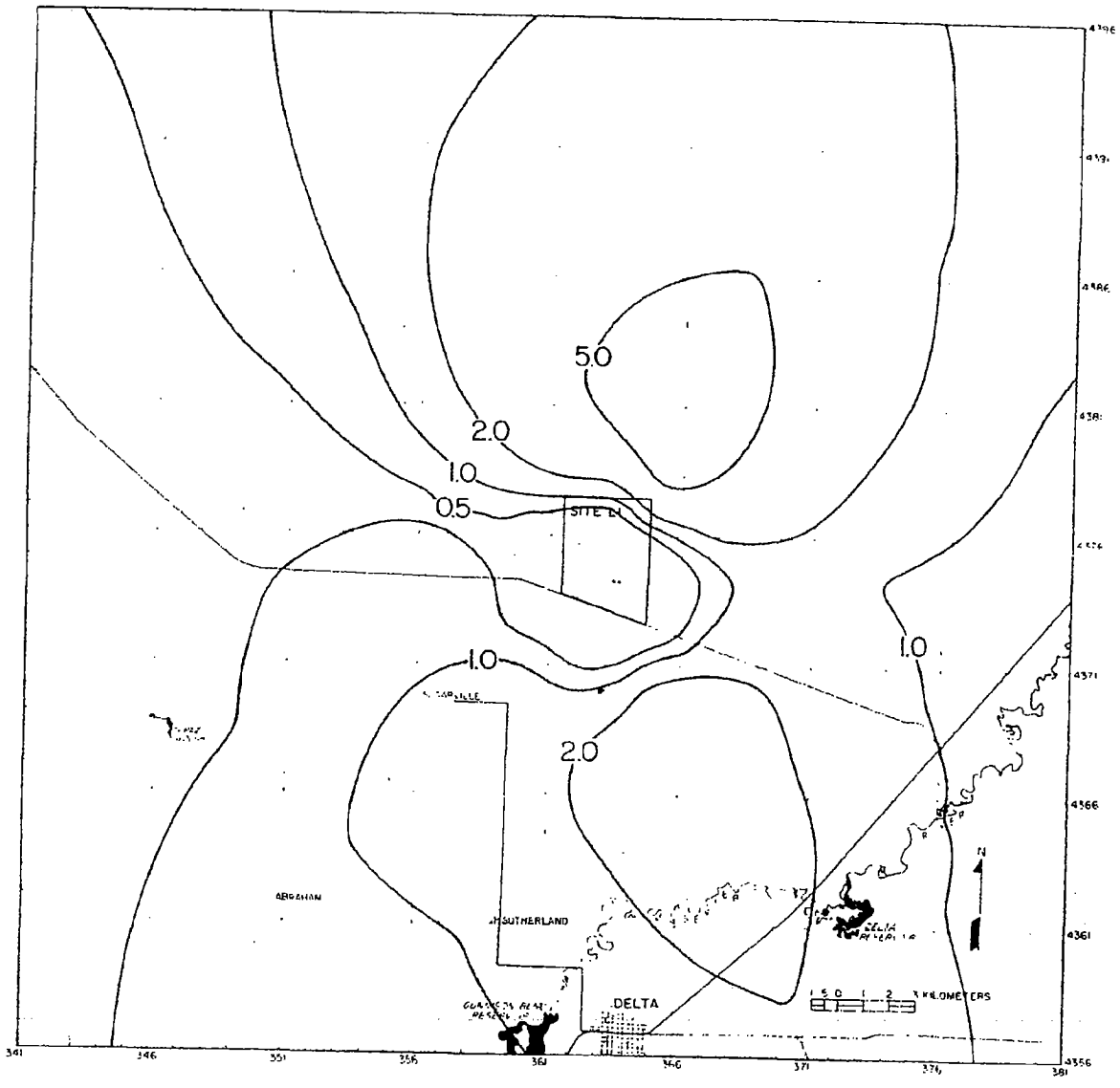

FIGURE 3-2. Calculated isopleths of annual average ground-level NO_2 concentration in micrograms per cubic meter for the IPP Power Plant located at site L1.

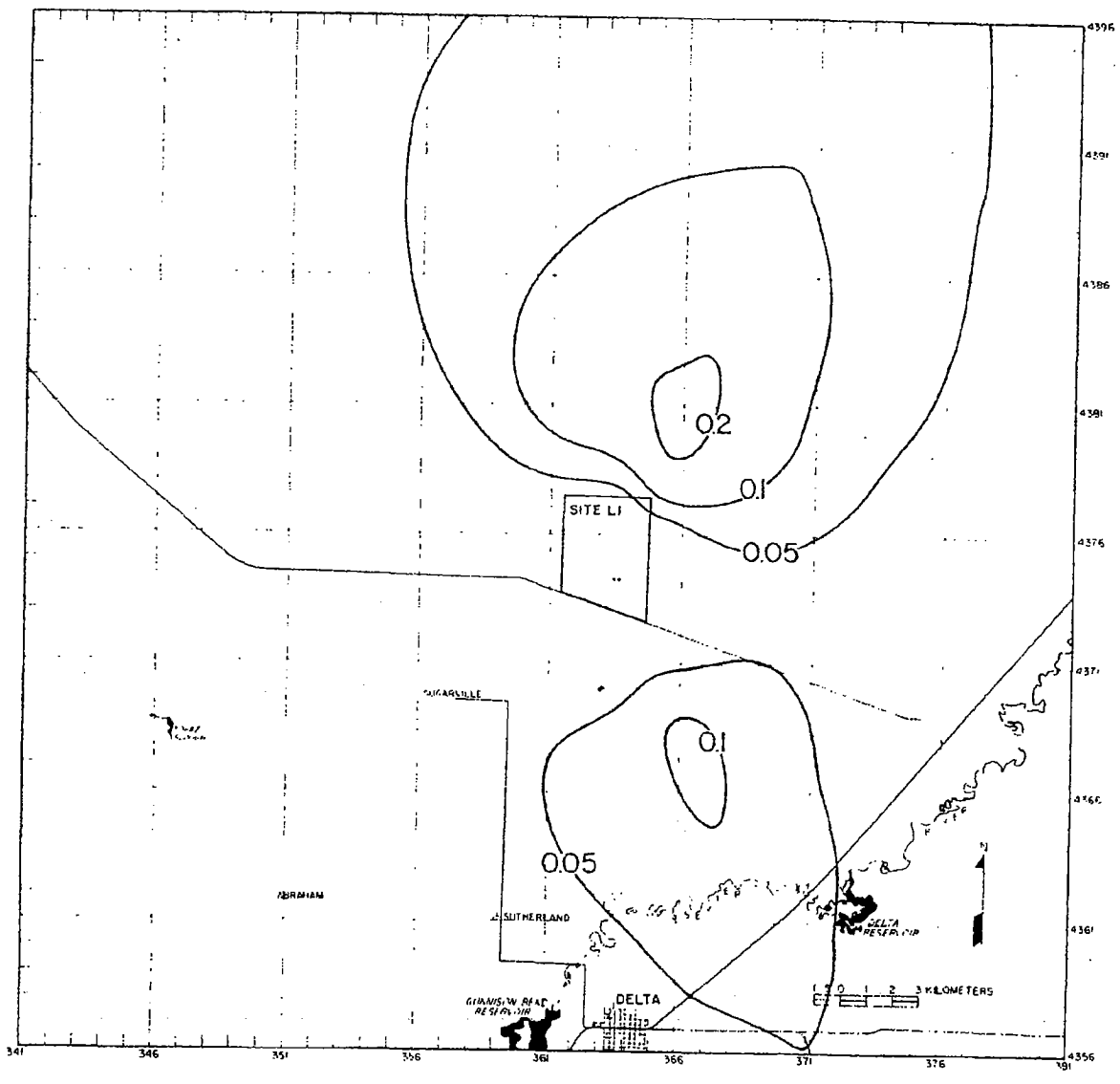

FIGURE 3-3. Calculated isopleths of annual average ground-level particulate concentration in micrograms per cubic meter for the IPP Power Plant located at site L1.

2.1, the NO_2 concentrations in Figure 3-2 and Table 3-1 may overestimate the NO_2 concentrations that can be expected to occur by as much as a factor of 10 because the calculations assumed that all of the NO is initially in the form of NO_2.

Annual SO_2 and particulate concentrations were also calculated for the Deep Creek Mountains potential Class I region (see Figure 1-1). As explained in Section 3.2.2, this is the only existing or potential Class I region likely to be affected by emissions from the IPP plant at site L1. Table 3-2 summarizes the results of the annual concentration calculations for the Deep Creek Mountains. The annual Class I Non-Deterioration Increments for SO_2 and particulates are 2 and 5 micrograms per cubic meter, respectively. The calculated maximum annual average SO_2 concentration of 0.016 micrograms per cubic meter is only about 0.8 percent of the annual Class I Increment for SO_2. Similarly, the calculated maximum annual average particulate concentration of 0.002 micrograms per cubic meter is only about 0.04 percent of the annual Class I Increment for particulates.

3.2 SHORT-TERM GROUND-LEVEL CONCENTRATIONS

The calculated short-term concentrations presented in this section are based on actual rather than hypothetical meteorological data. The 3-hour and 24-hour average ground-level concentrations given below are for the combinations of meteorological and topographic conditions that maximize the 3-hour and 24-hour average ground-level concentrations calculated following the short-term modeling procedures outlined in Sections A.3 and A.5 of Appendix A. The failure to refer explicitly in the following paragraphs to meteorological conditions other than the meteorological conditions associated with the highest calculated concentrations does not mean that other meteorological conditions were not considered. Based on our experience in modeling tall stack emissions for direct comparisons with observed air quality (for example, Cramer, 1976),

TABLE 3-1

MAGNITUDES AND LOCATION OF CALCULATED MAXIMUM ANNUAL AVERAGE GROUND-LEVEL SO_2, NO_2 AND PARTICULATE CONCENTRATIONS

Pollutant	Concentration ($\mu g/m^3$)	Location	
		Distance (km)	Bearing (deg)
SO_2	1.83	6.7	045
NO_2	8.28	6.7	045
Particulates	0.23	6.7	045

TABLE 3-2

MAXIMUM ANNUAL AVERAGE SO_2 AND PARTICULATE CONCENTRATIONS CALCULATED AT THE DEEP CREEK MOUNTAINS

Pollutant	Concentration ($\mu g/m^3$)
SO_2	0.016
Particulates	0.002

we have calculated maximum 3-hour and 24-hour average concentrations for the meteorological conditions that, in our opinion, are supported by both theory and air quality data as being the "worst-case" conditions.

3.2.1 Maximum Short-term Concentrations at Any Point

24-Hour Average Concentrations

For a power plant located in open terrain, both theory (Pasquill, 1974 and others) and air quality data (Gorr and Dunlap, 1977 and others) indicate that the highest 24-hour average ground-level concentrations occur during periods of persistent moderate-to-strong winds in combination with neutral stabilty. Additionally, following the terrain-adjustment procedures outlined in Section A.5 of Appendix A, the highest calculated 24-hour average concentrations for tall stack emissions usually occur when persistent moderate-to-strong winds blow toward nearby elevated terrain. In the case of site L1, significant elevated terrain features are so far from the plant site that the 24-hour average ground-level concentrations calculated for the elevated terrain are all considerably less than the maximum concentrations calculated in the immediate vicinity of the plant site during periods of persistent moderate-to-strong winds. We therefore selected a period of persistent moderate-to-strong south-southwest winds (2200 MST on 22 June 1950 to 2100 MST on 23 June 1950) as the "worst-case" 24-hour period for site L1. This is the same period that we selected as the "worst-case" 24-hour period for alternate site A6 in our previous calculations for BLM. Based on wind-persistence statistics for the Delta Airport, we believe that similar persistent wind conditions can be expected to occur about once per year.

The source data given in Section 2.1 and the hourly meteorological inputs for the "worst-case" 24-hour period given in Appendix B were used with the short-term concentration model described in Section A.3

of Appendix A to calculate hourly and 24-hour average ground-level concentrations of SO_2 and particulates. The procedures used to develop the hourly meteorological inputs are discussed in Section 2.2.3. Concentrations were calculated for the regularly-spaced grid described in Section 3.1 and for additional points spaced at 500-meter intervals along the trajectories defined by the most frequent wind directions. The procedures outlined in Section A.5 were used to account for the effects of variations in terrain height over the calculation grid.

The calculated isopleths of maximum 24-hour average ground-level concentrations of SO_2 and particulates are shown in Figures 3-4 and 3-5, respectively. Table 3-3 gives the magnitudes and location of the calculated maximum 24-hour average concentrations. The 24-hour Class II Non-Deterioration Increments for SO_2 and particulates are 91 and 37 micrograms per cubic meter, respectively. The calculated maximum 24-hour average SO_2 concentration of 50 micrograms per cubic meter is 55 percent of the 24-hour Class II Increment for SO_2 and the calculated maximum 24-hour average particulate concentration of 6 micrograms per cubic meter is 16 percent of the 24-hour Class II Increment for particulates.

3-Hour Average SO_2 Concentrations

The highest calculated 3-hour SO_2 concentrations at site L1 were associated with periods of persistent moderate-to-strong winds, periods of transition from a stable thermal stratification to an unstable thermal stratification or vice versa, and periods with limited mixing. We define limited mixing as a period of light-to-moderate winds in combination with neutral or slightly stable conditions with the IPP plumes contained within a relatively shallow mixing layer. This definition of limited mixing differs from the TVA definition (Carpenter, et al., 1971) which is restricted to daytime hours during periods of fair weather with light-to-moderate winds below an elevated subsidence inversion. We selected a limited-mixing case (2200 to 0000 MST on 1-2 December 1951)

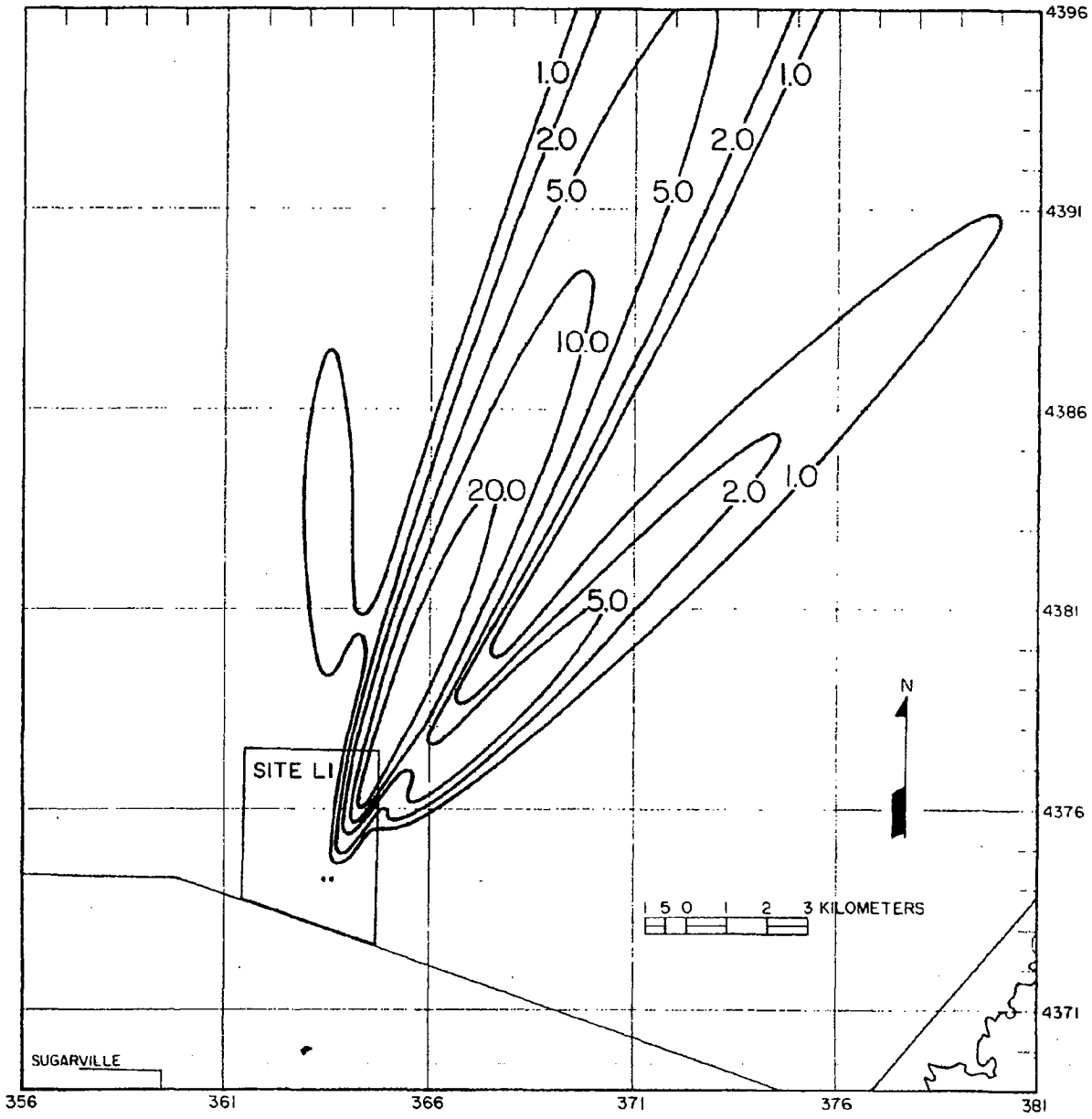

FIGURE 3-4. Calculated isopleths of maximum 24-hour average ground-level SO_2 concentration in micrograms per cubic meter for the IPP Power Plant located at site L1.

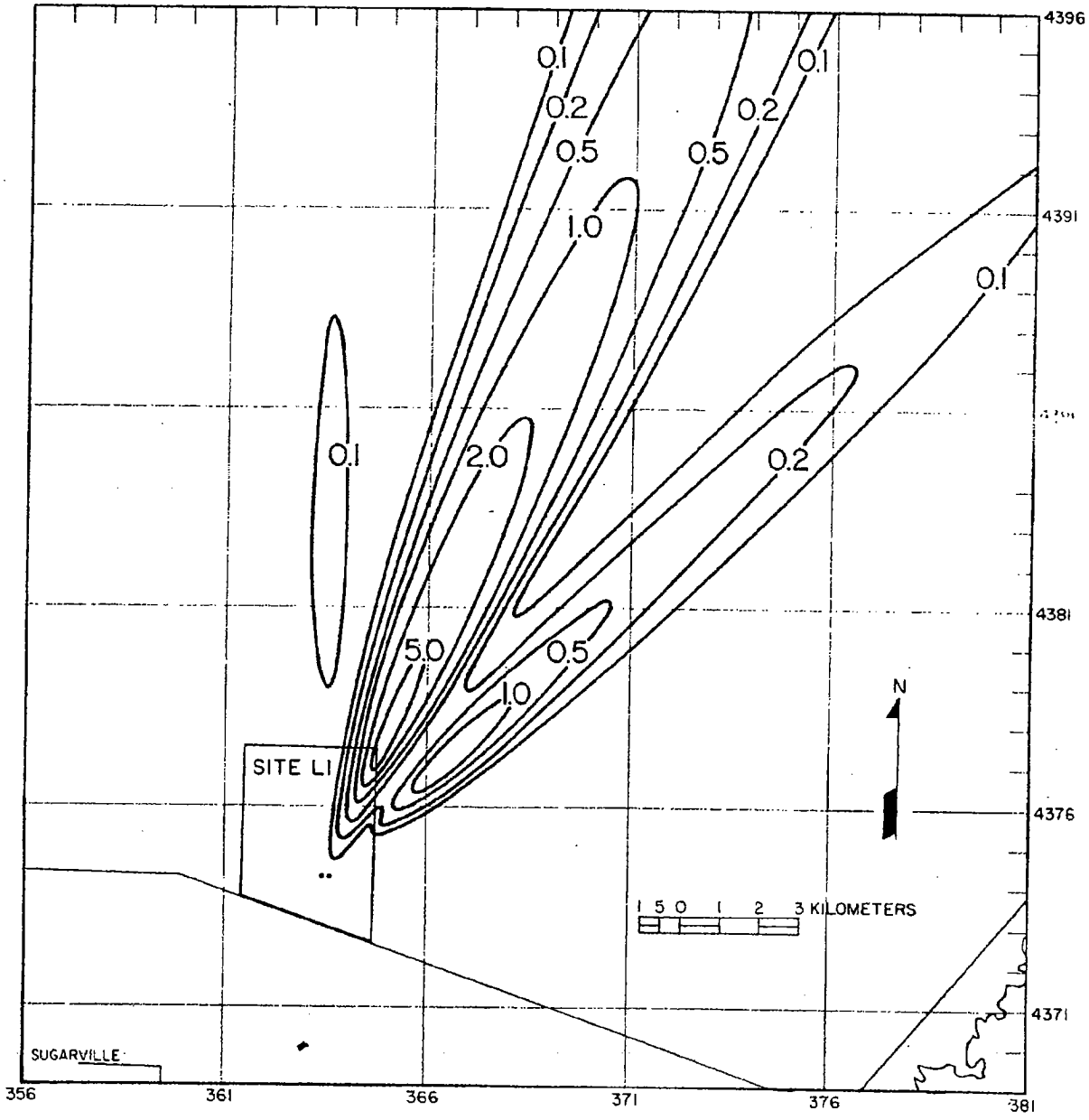

FIGURE 3-5. Calculated isopleths of maximum 24-hour average ground-level particulate concentration in micrograms per cubic meter for the IPP Power Plant located at site L1.

TABLE 3-3

MAGNITUDES AND LOCATION OF CALCULATED MAXIMUM 24-HOUR AVERAGE GROUND-LEVEL SO_2 AND PARTICULATE CONCENTRATIONS

Pollutant	Concentration ($\mu g/m^3$)	Location	
		Distance (km)	Bearing (deg)
SO_2	50	4.0	023
Particulates	6	4.0	023

as the "worst-case" 3-hour period for site L1. This is the same period that we selected as the "worst-case" 3-hour period for alternate site A6 in our previous calculations for BLM. The hourly meteorological inputs for this period are given in Appendix B. The calculation procedures are the same as those given above for the 24-hour concentration calculations.

Figure 3-6 shows the calculated isopleths of 3-hour ground-level SO_2 concentration for the "worst-case" 3-hour period. The calculated maximum 3-hour concentration of 138 micrograms per cubic meter is located approximately 8 kilometers north-northeast of the plant. This concentration is only about 27 percent of the 3-hour Class II SO_2 Increment of 512 micrograms per cubic meter. Based on the wind persistence statistics for the Delta Airport, 3-hour SO_2 concentrations on the order of 100 micrograms per cubic meter might occur about 200 times per year if the various meteorological regimes leading to relatively high 3-hour concentrations are considered.

An empirical check on the consistency of the calculated maximum 3-hour and 24-hour average SO_2 concentrations is the ratio of the calculated maximum 24-hour to maximum 3-hour SO_2 concentrations. Martin and Reeves (1977) give ratios of maximum 24-hour to maximum 3-hour SO_2 concentrations (running averages) for 33 air quality monitors located in the vicinity of large coal-fired power plants. They found that the mean ratios varied from 0.31 to 0.42. The model ratio for site L1 of 0.36 is in very good agreement with their results.

3.2.2 Maximum Short-Term Concentrations at Existing and Potential Class I Regions

As explained in Section 3.2.2 of our March 1978 report to BLM, we do not believe that emissions from the proposed IPP Power Plant at site L1 will have any significant effect on the ambient air quality at the existing and potential Class I regions in southeastern Utah. For example,

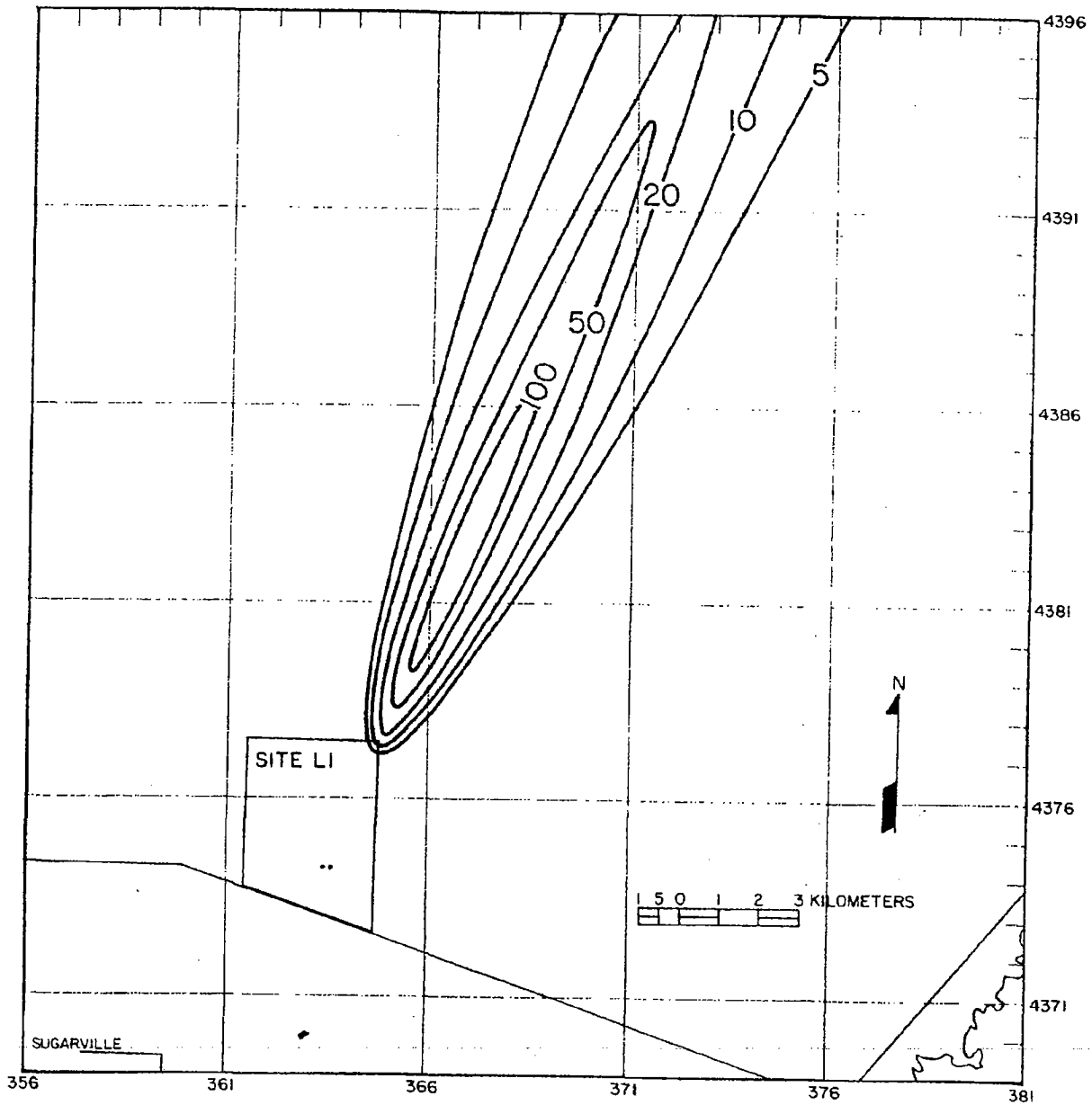

FIGURE 3-6. Calculated isopleths of maximum 3-hour average ground-level SO_2 concentration in micrograms per cubic meter for the IPP Power Plant located at site L1.

in order for emissions from the IPP plant located at site L1 to affect directly Capitol Reef National Park and the other existing and potential Class I regions in southeastern Utah, the IPP plumes must pass over the Wasatch Plateau, which extends to about 3,350 meters above mean sea level. It follows that the minimum mixing depth required for the IPP plumes to clear the Wasatch Plateau is about 2,000 meters. As shown by Table 2-7, the lowest wind-speed category with a median mixing depth of 2,000 meters is the category for wind speeds less than or equal to 1.5 meters per second during spring afternoons. Assuming C stability (the most stable Pasquill stability category consistent with a 2,000-meter mixing depth), a wind speed of 1.5 meters per second and the other meteorological parameters assigned to this combination of wind-speed and stability categories (see Tables 2-5, 2-6, 2-8 and 2-9), the maximum 1-hour ground-level SO_2 concentration calculated at the nearest boundary of Capitol Reef is only 4 micrograms per cubic meter. The 3-hour and 24-hour Class I SO_2 Increments are 25 and 5 micrograms per cubic meter, respectively. Thus, under worst-case meteorological conditions, the effects of emissions from the IPP plant located at site L1 on the ambient air quality of southeastern Utah will be negligible. The only existing or potential Class I region that we believe might be affected by emissions from the IPP plant at site L1 is the Deep Creek Mountains potential Class I region (see Figure 1-1).

Section 2.2.3 outlines the procedures used to select the "worst-case" 3-hour and 24-hour periods for emissions from the IPP plant at the Deep Creek Mountains potential Class I region. The hourly meteorological inputs for these periods are given in Appendix B. The short-term concentration model described in Section A.3, including the terrain-adjustment procedures outlined in Section A.5, was used to calculate concentrations at and beyond the intersections of the boundary of the potential Class I region with the straight-line plume trajectories defined by the most frequent wind directions. No attempt was made to take into account the time required for the downwind transport of emissions

from the IPP Power Plant to the potential Class I region. That is, the plumes were assumed to pass over the Deep Creek Mountains whenever the wind direction was toward the Deep Creek Mountains. Additionally, we did not consider the possibility of chemical transformations or other removal processes (the decay constant ψ in Equation (A-9) was set equal to zero). Thus, the calculation procedures were biased toward overestimation at the longer downwind distances.

Table 3-4 summarizes the results of the short-term SO_2 and particulate concentration calculations for the Deep Creek Mountains potential Class I region. The calculated maximum 3-hour SO_2 concentration of 17.3 micrograms per cubic meter is 69 percent of the 3-hour Class I SO_2 Increment, while the calculated maximum 24-hour SO_2 concentration of 2.8 micrograms per cubic meter is 56 percent of the 24-hour Class I SO_2 Increment. Similarly, the calculated maximum 24-hour particulate concentration of 0.4 micrograms per cubic meter is about 4 percent of the 24-hour Class I Increment for particulates of 10 micrograms per cubic meter. Thus, the results of the short-term concentration calculations described in this section in combination with the results of the annual concentration calculations described in Section 3.1 indicate that the proposed IPP Power Plant at site L1 can meet Class I requirements at all existing and potential Class I regions.

3.3 POSSIBLE INTERACTIONS WITH OTHER SOURCES

As noted in Section 1.3, there are no significant stationary sources of air pollutants in the vicinity of the Lynndyl site (IPP site L1). The nearest major pollutant sources are located along the industrialized Wasatch Front (Utah, Salt Lake and Tooele counties) and include a copper smelter located 140 kilometers north-northeast of site L1 and a steel works located about 115 kilometers northeast of site L1.

TABLE 3-4

MAXIMUM SHORT-TERM SO_2 AND PARTICULATE CONCENTRATIONS CALCULATED AT THE DEEP CREEK MOUNTAINS POTENTIAL CLASS I REGION

Averaging Time	Concentration ($\mu g/m^3$)	
	SO_2	Particulates
3 Hours	17.3	--
24 Hours	2.8	0.4

The mountain ranges in Utah effectively form functional air basins with minimal exchange at the boundaries of adjacent air basins except during periods of high dilution conditions (moderate-to-strong winds and/or deep surface mixing layers). Also, because of the general north-south orientation of the mountain ranges, there is very little east-west or west-east transport within the surface mixing layer. For example, during the period when the copper smelter located on the west side of the Salt Lake Valley was closed by a strike, there was no decrease in the SO_2 concentrations measured on the east side of the valley (Hill, 1972). As explained in Section 1.3, we believe that significant interactions of emissions from the IPP Power Plant at site L1 with emissions from the copper smelter, steel works and other pollutant sources along the Wasatch Front are unlikely because, in our opinion, site L1 and the Wasatch Front are in different functional air basins. Additionally, the east-west separation between site L1 and the major pollutant sources along the Wasatch Front is over 50 kilometers.

The current Prevention of Significant Deterioration (PSD) Regulations (Federal Register, Vol. 43, No. 118, p. 26398) define the amount of ambient impact that is significant as:

- Annual SO_2 and/or particulate concentrations above 1 microgram per cubic meter
- Twenty-four-hour SO_2 and/or particulate concentrations above 5 micrograms per cubic meter
- Three-hour SO_2 concentrations above 25 micrograms per cubic meter

The calculations described in Sections 3.1 and 3.2 indicate that, with the exception of short-term SO_2 concentrations, the proposed IPP Power Plant will not have a significant air quality impact (following the

definition of a significant impact given above) at distances beyond about 10 to 20 kilometers from the plant. Because significant short-term SO_2 concentrations are possible beyond 20 kilometers, we calculated maximum short-term SO_2 concentrations for Tooele, the nearest location at which violations of the National Ambient Air Quality Standards (NAAQS) for SO_2 were observed during 1977.

The Tooele SO_2 monitoring site is about 115 kilometers north-northeast of site L1. With the exception of mixing depths, we selected the "worst-case" 3-hour and 24-hour periods for Tooele following the same procedures given in Section 2.2.3 for the Deep Creek Mountains potential Class I region. Because emissions from the IPP Power Plant at site L1 must pass over the Sheep Rock Mountains in order to affect directly the Tooele monitor, we assumed that the mixing depth must be at least 800 meters. The hourly meteorological inputs for the "worst-case" 3-hour and 24-hour periods are given in Appendix B. The calculation procedures are the same as the procedures described in Section 3.2.2 for the Deep Creek Mountains.

The maximum 3-hour and 24-hour average SO_2 concentrations calculated for the Tooele SO_2 monitor as a result of emissions from the proposed IPP Power Plant at site L1 are 7.9 and 2.5 micrograms per cubic meter, respectively. As noted above, EPA considers significant 3-hour and 24-hour SO_2 concentration contributions to be 25 and 5 micrograms per cubic meter, respectively. Thus, under "worst-case" meteorological conditions, the plant's calculated air quality impact at Tooele is not significant.

According to the Utah Bureau of Air Quality, the 3-hour NAAQS for SO_2 of 1,300 micrograms per cubic meter was exceeded at the Tooele monitor twice during 1977, while the 24-hour NAAQS for SO_2 of 365 micrograms per cubic meter was exceeded on three days during 1977. Inspection of surface weather maps for the dates of violations of the 3-hour

standard (14 April and 16 October) and for the dates of violations of the 24-hour standard (16 October, 11 November and 10 December) indicate that the violations occurred during periods with an elevated subsidence inversion and north to northeast winds that would transport emissions from the copper smelter to the Tooele monitor or during periods of poor dilution conditions (light and variable winds and shallow mixing depths) when the low-level emissions from the copper smelter would tend to fill the Rush Valley.

The maximum 3-hour SO_2 concentration observed during 1975 at the Tooele monitor was 2,175 micrograms per cubic meter, or 167 percent of the 3-hour standard, and the maximum observed 24-hour SO_2 concentration was 445 micrograms per cubic meter, or 122 percent of the 24-hour standard. Assuming the copper smelter to be the principal cause of the observed SO_2 concentrations and assuming that the SO_2 concentrations are approximately inversely related to distance from the smelter at downwind distances beyond Tooele, the maximum 3-hour and 24-hour SO_2 concentrations at site L1 are 360 and 74 micrograms per cubic meter, respectively. If the maximum 3-hour and 24-hour SO_2 concentrations calculated for the IPP Power Plant are added to these concentrations, the resulting 3-hour and 24-hour SO_2 concentrations are 498 and 124 micrograms per cubic meter, respectively. Thus, the combination of the maximum short-term SO_2 concentrations calculated for the IPP Power Plant at site L1 with the maximum observed SO_2 concentrations at the Tooele monitor, extrapolated to site L1, leads to short-term SO_2 concentrations that are well below the short-term NAAQS for SO_2. However, the maximum concentrations calculated for site L1 and the high observed SO_2 centrations at Tooele occurred under different meteorological conditions. As indicated above, we doubt that significant interactions between the air basin containing the copper smelter and the Tooele monitor and the air basin containing site L1 actually occurred during the periods of highest observed SO_2 concentrations at the Tooele monitor. Additionally, we point out that the smelter has recently converted to the Noranda smelting process, significantly decreased low-level fugitive

emissions and switched from two 122-meter stacks to a single 380-meter stack. Both the smelter and the Utah Bureau of Air Quality believe that these changes will prevent violations of the NAAQS for SO_2 as a result of the smelter's emissions.

In summary, we believe that significant interactions of emissions from the proposed IPP Power Plant located at site L1 with emissions from stationary pollutant sources located along the Wasatch Front are unlikely because site L1 and the Wasatch Front area are contained in different functional air basins. Following the EPA definition of a significant air quality impact, the results of our model calculations indicate that the plant will not have a significant impact at the nearest representative air quality monitoring sites where violations of the NAAQS have been measured. Also, extrapolation of the maximum observed SO_2 concentrations for the nearest monitoring site at which violations of the NAAQS for SO_2 have been measured to the area of maximum impact for the IPP plant at site L1 indicate that emissions from the plant will not endanger the NAAQS for SO_2. Finally, we point out that, with the exception of Class I regions, EPA does not intend to apply air quality models at downwind distances greater than 50 kilometers because of the uncertainty in model calculations at long downwind distances (Federal Register, Vol. 43, No. 118, p. 26398). The distance from site L1 to the nearest major stationary pollutant source is more than double this threshold distance.

SECTION 4
CONCLUSIONS

4.1 SUMMARY OF THE RESULTS OF THE CALCULATIONS

Table 4-1 lists the magnitudes and locations of the maximum short-term and annual average ground-level concentrations of SO_2, NO_2 and particulates calculated for the proposed IPP Power Plant at the Lynndyl site (IPP site L1). The National Ambient Air Quality Standards (NAAQS) and the Class I and Class II Non-Deterioration Increments are listed in Table 4-2. The area surrounding site L1 is a Class II (moderate air quality deterioration permitted) region. Comparison of the results of the diffusion-model calculations in Table 4-1 with Table 4-2 shows that emissions from the proposed IPP Power Plant at site L1 will not endanger any National Ambient Air Quality Standard or Class II Non-Deterioration Increment. The results of the model calculations also show that the only existing or potential Class I (pristine air quality) region likely to be affected by emissions from the IPP Plant located at site L1 is the Deep Creek Mountains potential Class I region, located 107 kilometers west of site L1. The maximum short-term and annual average SO_2 and particulate concentrations calculated for the Deep Creek Mountains are given in Table 4-3. As shown by a comparison of Tables 4-2 and 4-3, emissions from the proposed IPP Power Plant at site L1 will not endanger the Class I Non-Deterioration Increments at the Deep Creek Mountains.

On the basis of our analysis of topographic, meteorological and air quality data, we believe that significant interactions of emissions from the proposed IPP Power Plant at site L1 with emissions from the pollutant sources along the industrialized Wasatch Front area are unlikely because site L1 and the Wasatch Front area are contained in different functional air basins. Also, following the EPA definition of a significant air quality impact, the results of our diffusion-model

TABLE 4-1

MAGNITUDES AND LOCATIONS OF CALCULATED MAXIMUM SHORT-TERM AND ANNUAL AVERAGE SO_2, NO_2 AND PARTICULATE CONCENTRATIONS FOR THE IPP POWER PLANT AT SITE L1

Averaging Time	Concenration (μg/m)			Location	
	SO_2	NO_2	Particulates	Distance (km)	Bearing (deg)
3 Hours	138	--	--	8.0	023
24 Hours	50	--	6	4.0	023
Annual	1.83	8.28*	0.23	6.7	045

*The calculated annual NO_2 concentration assumes that 100-percent of the NO contained in the flue gas is converted to NO_2.

TABLE 4-2

NATIONAL AMBIENT AIR QUALITY STANDARDS
AND NON-DETERIORATION INCREMENTS

Pollutant	Averaging Time	National Ambient Air Quality Standard ($\mu g/m^3$)	Non-Deterioration Increment ($\mu g/m^3$)	
			Class I	Class II
SO_2	3 Hours	1,300	25	512
	24 Hours	365	5	91
	Annual	80	2	20
Particulates	24 Hours	260 (150)*	10	37
	Annual**	75 (60)*	5	19
NO_2	Annual	100	--	--

*The secondary particulate standards are enclosed by parentheses.
**Annual geometric mean.

TABLE 4-3

MAXIMUM SHORT-TERM AND ANNUAL AVERAGE SO_2 AND PARTICULATE CONCENTRATIONS CALCULATED AT THE DEEP CREEK MOUNTAINS

Averaging Time	Concentration ($\mu g/m^3$)	
	SO_2	Particulates
3 Hour	17.3	--
24 Hour	2.8	0.4
Annual	0.016	0.002

calculations indicate that the plant will not have a significant impact at the nearest representative air quality monitoring sites where violations of the National Ambient Air Quality Standards have been measured.

The accuracy of the diffusion models used in this study should be considered in assessing compliance with the National Ambient Air Quality Standards and the Class I and Class II Non-Deterioration Increments. In validation studies for SO_2 sources located in complex terrain, the short-term and long-term diffusion models used in this study have, on the average, calculated SO_2 concentrations within 20 percent of the observed values for all averaging times at distances ranging from about 1 to 30 kilometers from the source (see Section 4.2 and Appendix D of our report to BLM). The accuracy of the models has not been established at distances greater than about 30 kilometers. Also the results of the model calculations are biased toward overestimation at the longer downwind distances because of the neglect of transport time and the assumed absence of any SO_2 depletion by chemical transformations or surface deposition.

4.2 IDENTIFICATION OF THE MAJOR AREAS OF UNCERTAINTY IN THE DIFFUSION-MODEL CALCULATIONS

The principal areas of uncertainty affecting the accuracy of the diffusion-model calculations described in this report are:

- The representativeness of the emissions data and stack parameters given in Section 2.1 for the proposed IPP Power Plant

- The representativeness of the meteorological inputs used in the calculations

- The accuracy of the short-term and long-term diffusion models used in the calculations, including the procedures used to account for the effects of elevated terrain on ground-level concentrations

We have no basis for assessing the representativeness of the source parameters and emissions data provided by IPP and used in the diffusion-model calculations. However, the source and emissions data given in Section 2.1 are consistent with the corresponding data that we have seen for other coal-fired power plants proposing to use electrostatic precipitators and a flue gas desulfurization system.

We selected what we consider to be the best available data to develop the meteorological inputs used in our diffusion-model calculations for the proposed IPP Power Plant at the Lynndyl site (IPP site L1). Because of the close proximity of site L1 to the Delta, Utah Airport, we believe that the Delta Airport surface weather observations are representative of conditions at site L1. On the basis of our experience at Dugway Proving Ground and the isopleths of mean mixing depths given by Holzworth (1972), we also believe that the Salt Lake City mixing depths used in the calculations for site L1 are sufficiently representative of the site for use in an air quality impact analysis. The procedures that we used to assign turbulent intensities (i.e., dispersion coefficients) are the same as the procedures that we have used in many of our model validation studies. As indicated below, these procedures have resulted in good agreement between calculated and measured air quality for SO_2 sources located in complex terrain. The other meteorological inputs (wind-profile exponents and vertical potential temperature gradients) were based on measurements at similar locations and are believed to be representative of conditions in the vicinity of site L1.

It is not possible to demonstrate the accuracy of our diffusion-model calculations for the proposed IPP Power Plant at site L1 by means of direct comparisons of concurrent calculated and observed concentrations. However, on the basis of recent studies for the U. S. Environmental Protection Agency (EPA) of SO_2 sources located in complex terrain (see Appendix D of our March 1978 report to BLM), we can specify approximate confidence intervals for our model predictions. Confidence intervals, in contrast to confidence limits which must satisfy strict statistical criteria, simply reflect the results of direct comparisons of model predictions with air quality observations without attempting to account for the effects of sample size and other limitations as must be done in the case of estimating confidence limits. In the cases where the plume from an isolated source was simultaneously detected by two or more SO_2 monitors which allowed us to specify the wind direction at the plume height to within 1 or 2 degrees, our short-term model yielded calculated hourly SO_2 concentrations that were, on the average, equal to the observed concentrations (see Cramer, et al., 1977). Individual calculated and observed hourly SO_2 concentrations differed by as much as a factor of two or more. To a large extent, we believe that the discrepancies between the individual calculated and observed hourly concentrations were caused by random errors in the model input data (source and meteorological) and in the air quality measurements. When unadjusted surface wind directions were used in our model calculations, the calculated maximum 3-hour and 24-hour average SO_2 concentrations were, on the average, within 20 percent of the observed values (see Section 8 of Cramer, et al., 1975). Our long-term diffusion model has yielded calculated annual average SO_2 concentrations within 10 percent of the observed values at all monitors where the annual average SO_2 concentrations were above the accuracy and threshold of the monitors (Cramer, et al., 1975). In cases where the annual average SO_2 concentrations were below the threshold of the SO_2 monitors, our long-term model has yielded calculated annual average SO_2 concentrations that were within plus or minus one-half the accuracy and threshold of the SO_2 instrument

(for example, see Cramer, et al., 1976). However, we point out that we have no model validation data at downwind distances greater than about 30 kilometers. The concentrations calculated at distances beyond about 30 kilometers are thus subject to more uncertainty that the concentrations calculated in the vicinity of site L1. Also, the calculation procedures for these longer distances tend to be biased toward overestimation.

In summary, we believe that the results of the concentration calculations presented in this report provide a realistic assessment of the potential air quality impact of stack emissions from the proposed IPP Power Plant located at site L1. The hourly surface weather observations for the nearby Delta, Utah Airport for the 6-year period 1949 through 1954 form a data base that is unusually comprehensive for a remote location. The other meteorological inputs used in the model calculations are based on measurements at similar locations and are believed to be representative of conditions at site L1. Also, our models have yielded a good correspondence between concurrent calculated and observed concentrations (at distances up to 30 kilometers from the source) for SO_2 sources located in terrain of greater complexity than the terrain within a 30-kilometer radius of site L1.

REFERENCES

Berman, E. A. and R. Baskett, 1976: Regional air quality analysis in the State of Utah and surrounding regions. ERT Document No. P-5-34-4 (Revised July 1977), prepared for U. S. Department of the Interior, Bureau of Land Management, Denver, Colorado.

Bowers, J. F., H. E. Cramer and A. J. Anderson, 1978: Final report: assessment of the air quality impact of emissions from the proposed IPP Power Plant at the primary and six alternate sites. H. E. Cramer Company, Inc. Technical Report TR-78-311-01, prepared for U. S. Department of the Interior, Bureau of Land Management, Denver, Colorado.

Bowers, J. F. and H. E. Cramer, 1976: Comparison of calculated and observed characteristics of plumes from two coal-fired power plants located in complex terrain. Paper presented at the Third Symposium on Atmospheric Turbulence, Diffusion and Air Quality, Raleigh, N. C. October 19-22, 1976.

Briggs, G. A., 1971: Some recent analyses of plume rise observations. In Proceedings of the Second International Clean Air Congress, Academic Press, New York.

Briggs, G. A., 1972: Chimney plumes in neutral and stable surroundings. Atm. Env., 6(7), 507-510.

Calder, K. L., 1971: A climatological model for multiple source urban air pollution. Proc. 2nd Meeting of the Expert Panel on Air Pollution Modeling. NATO Committee on the Challenges of Modern Society, Paris, France, July 1971, 33.

Carpenter, S. B., T. L. Montgomery, J. M. Leavitt, W. C. Colbaugh and F. W. Thomas, 1971: Principal plume dispersion models: TVA power plants. Journal of the Air Pollution Control Association, 21(8), 491-495.

Cramer, H. E., et al., 1972: Development of dosage models and concepts. Final Report under Contract DAAD09-67-C-0020(R) with the U. S. Army, Deseret Test Center Report DTC-TR-72-609, Fort Douglas, Utah.

Cramer, H. E., H. V. Geary and J. F. Bowers, 1975: Diffusion-model calculations of long-term and short-term ground-level SO_2 concentrations in Allegheny County, Pennsylvania. H. E. Cramer Company Technical Report TR-75-102-01 prepared for the U. S. Environmental Protection Agency, Region III, Philadelphia, Pennsylvania. EPA Report 903/9-75-018. NTIS Accession No. PB-245262/AS.

Cramer, H. E., 1976: Improved techniques for modeling the dispersion of tall stack plumes. Paper presented at the Seventh NATO/ CCMS International Technical Meeting on Air Pollution Modeling and its Application, Arlie, Virginia, 7-10 September 1976.

Cramer, H. E., J. F. Bowers and H. V. Geary, 1976: Assessment of the air quality impact of SO_2 emissions from the ASARCO-Tacoma smelter. EPA Report No. EPA 910/9-76-028. U. S. Environmental Protection Agency, Region X, Seattle, Washington.

Cramer, H. E., J. F. Bowers and H. V. Geary, 1977: Comparison of calculated and observed hourly ground-level SO_2 concentrations for the ASARCO-Tacoma copper smelter. APCA Paper No. 77-58.3 presented at the 70th Annual Meeting of the Air Pollution Control Association, Toronto, Ontario, Canada, June 20-24, 1977.

DeMarrais, G. A., 1959: Wind speed profiles at Brookhaven National Laboratory. J. Met., 16, 181-190.

Environmental Data Service, 1966: Tabulation I, Frequency of occurrence, average wind speed through mixing depth for Grand Junction, Colorado. Job No. 6234. National Climatic Center, Federal Building, Asheville, N. C.

Environemtal Data Service, 1968: Tabulation I, Frequency of occurrence, average wind speed through mixing depth for Salt Lake City, Utah. Job No. 6234. National Climatic Center, Federal Building, Asheville, N. C.

Gorr, W. L. and R. W. Dunlap, 1977: Characterization of steady wind incidents for air quality management. Atm. Env., 11, 59-64.

Hill, A. C., et al., 1976: Vegetation and air quality environmental studies for the North Emery Power Plant Site, progress report-1974. University of Utah Research Institute Report, prepared for Utah Power and Light Company, Salt Lake City, Utah.

Hill, G. R., 1972: The hazards of SO_2 in the Salt Lake Valley-myth or reality. Bulletin No. 141 of the Utah Engineering Station, Vol. 63, No. 19, University of Utah, Salt Lake City, Utah.

Holzworth, G. C., 1972: Mixing heights, wind speeds and potential for urban air pollution throughout the continguous United States. USEPA, OAP, Research Triangle Park, N. C., Publication No. AP-101.

Huber, A.H. and W. H.Snyder, 1976: Building wake effects on short stack effluents. Paper Presented at the Third Symposium on Atmospheric Turbulence, Diffusion and Air Quality. Raleigh, North Carolina, October 19-22, 1976.

Luna, R. E. and H. W. Church, 1971: A comparison of turbulence intensity and stability ratio measurements to Pasquill turbulence types. Paper presented at a Conference on Air Pollution Meteorology, Raleigh, N. C., April 5-9, 1971.

Martin, J. R. and R. W. Reeves, 1977: Relationships among observed short-term maximum sulfur dioxide concentrations near coal-fired power plants. APCA Paper N. 77-29.5 presented at the 70th Annual Meeting of the Air Pollution Control Association, Toronto, Ontario, Canada, June 20-24, 1977.

Ogren, J. A., D. L. Blumenthal and A.H. Vanderpol, 1977: Oxidant measurements in western power plant plumes. EPRI EA-421 Research Project 861-1), Electric Power Research Institute Palo Alto, California.

Osipov, Y. S., 1972: Diffusion from a point source of finite time of action. In AICE Survey of USSR Air Pollution Literature-Volume XII, distributed by National Technical Information Service, Springfield, Virginia.

Pasquill, F., 1961: The estimation of the dispersion of windborne material. Met. Mag., 90, 33-49.

Pasquill, F., 1962: Atmospheric Diffusion. D. Van Nostrand Co., Ltd., London, 297.

Pasquill, F., 1974: Atmospheric Diffusion (Second Edition). Ellis Horwood Limited, Sussex, England, 429.

Record, F. A., et al., 1975: Field studies of suspended particulates in two Idaho cities. APCA Paper No. 75-28.2 presented at the 68th Annual Meeting of the Air Pollution Control Association, Boston, Mass., June 15-20, 1975.

Touma, J. S., 1977: Dependence of the wind profile power law on stability for various locations. Journal of the Air Pollution Association, 27(9), 863-866.

Turner, D. B., 1964: A diffusion model for an urban area. Journal of Applied Meteorology, 3(1), 83-91.

APPENDIX A

MATHEMATICAL MODELS USED TO CALCULATE GROUND-LEVEL CONCENTRATIONS

A.1 INTRODUCTION

The computerized diffusion models described in this appendix fall into two general categories: (1) Short-term models for calculating time-averaged ground-level concentrations for averaging times of 1, 3, 8 and 24 hours; (2) Long-term models for calculating seasonal and annual ground-level concentrations. Both the short-term and long-term concentration models are modified versions of the Gaussian plume model for continuous sources described by Pasquill (1962). In the short-term model, the plume is assumed to have Gaussian vertical and lateral concentration distributions. The long-term model is a sector model similar in form to the Environmental Protection Agency's Climatological Dispersion Model (Calder, 1971) in which the vertical concentration distribution is assumed to be Gaussian and the lateral concentration distribution within a sector is rectangular (a smoothing function is used to eliminate sharp discontinuities at the sector boundaries). Vertical plume growth (σ_z) in the short-term and long-term models and lateral plume growth (σ_y) in the short-term model are calculated by using turbulent intensities in simple power-law expressions that include the effects of initial source dimensions. In both the short-term and long-term models, buoyant plume rise is calculated by means of the Briggs (1971; 1972) plume-rise formulas, modified to include the effects of downwash in the lee of the stack during periods when the wind speed at stack height equals or exceeds the stack exit velocity. An exponent law is used to adjust the surface wind speed to the source height for plume-rise calculations and to the plume stabilization height for the concentration calculations. Both the short-term and the long-term models contain provisions to account for the effects of complex terrain.

Table A-1 lists the hourly meteorological inputs required by the short-term concentration model. Lateral and vertical turbulent intensities σ'_A and σ'_E may be directly specified or may be assigned on the basis of the Pasquill stability category (see Section 3 of Cramer, et al., 1975). The Pasquill stability category is determined from surface weather observations using the Turner (1964) wind-speed and solar-index values. Mixing depths may be obtained from rawinsonde or pibal measurements, or they may be assigned on the basis of tabulations of the frequency of occurrence of wind speed and mixing depth (available from the National Climatic Center for synoptic rawinsonde stations). Potential temperature gradients may be obtained from measurements or assigned on the basis of climatology.

Table A-2 lists the meteorological inputs required by the long-term concentration model. Joint-frequency distributions of wind-speed and wind-direction categories, classified according to the Pasquill stability categories, are available from the National Climatic Center. Alternately, surface wind observations may be analyzed to generate wind-frequency distributions by time-of-day categories (night, morning, afternoon and evening). Vertical turbulent intensities may be determined from a climatology of actual measurements or may be assigned on the basis of the Pasquill stability categories. Median mixing depths may be determined from the seasonal tabulations of the frequency of occurrence of wind speed and mixing depth prepared by the National Climatic Center. Vertical potential temperature gradients may be assigned to the combinations of wind-speed and stability or time-of-day categories on the basis of climatology.

Table A-3 lists the source input parameters required by the short-term and long-term diffusion models. As shown by the table, the computerized short-term and long-term models calculate ground-level concentrations produced by emissions from stacks, building vents and roof monitors, and from area sources. Both the short-term and long-term models also use a Cartesian coordinate system (usually the Universal Transverse Mercator system) with the positive X axis directed toward the east and the positive Y axis directed toward the north.

TABLE A-1

HOURLY METEOROLOGICAL INPUTS REQUIRED BY THE SHORT-TERM CONCENTRATION MODEL

Parameter	Definition
$\bar{u}_R$	Mean wind speed at height z_R
θ	Mean wind direction at height z_R
p	Wind-profile exponent
σ'_A	Wind azimuth-angle standard deviation in radians
σ'_E	Wind elevation-angle standard deviation in radians
T_a	Ambient air temperature (^oK)
H_m	Depth of surface mixing layer
$\frac{\partial\theta}{\partial z}$	Vertical potential temperature gradient

TABLE A-2

METEOROLOGICAL INPUTS REQUIRED BY THE
LONG-TERM CONCENTRATION MODEL

Parameter	Definition
$f_{i,j,k,\ell}$ (Table)	Frequency distribution of wind-speed and wind-direction categories by stability or time-of-day categories for the ℓ^{th} season
z_R	Height at which wind-frequency distributions were obtained
$p_{k,i}$ (Table)	Wind-profile exponents for each stability or time-of-day category and i^{th} wind-speed category
$\sigma'_{E;i,k}$ (Table)	Standard deviation of the wind-elevation angle in radians for the i^{th} wind-speed category and k^{th} stability or time-of-day category
$T_{a;k,\ell}$ (Table)	Ambient air temperature for the k^{th} stability or time-of-day category and ℓ^{th} season
$\left(\frac{\partial\theta}{\partial z}\right)_{i,k}$ (Table)	Vertical potential temperature gradient for the i^{th} wind-speed category and k^{th} stability or time-of-day category
$H_{m;i,k,\ell}$ (Table)	Median surface mixing depth for the i^{th} wind-speed category, k^{th} stability or time-of-day category and ℓ^{th} season
$\bar{u}\{z_R\}_i$ (Table)	Mean wind speeds at height z_R

TABLE A-3

SOURCE INPUTS REQUIRED BY THE SHORT-TERM AND LONG-TERM CONCENTRATION MODELS

Parameter	Definition
Stacks	
Q	Pollutant emission rate
X, Y	X and Y coordinates of the stack
z_s	Elevation above mean sea level of the base of the stack
h	Stack height
v	Actual volumetric emission rate
T_s	Stack exit temperature
r	Stack inner radius
Building Sources	
Q	Pollutant emission rate
X, Y	X and Y coordinates of the center of the building
z_s	Elevation above mean sea level of the base of the building
h	Building height
L	Building length
W	Building width
δ	Angle measured clockwise between north and the long side of the building
Area Sources	
Q	Pollutant emission rate
X, Y	X and Y coordinates of the center of the area source
z_s	Elevation above mean sea level of the area source

TABLE A-3 (Continued)

Parameter	Definition
Area Sources (Continued)	
h	Characteristic vertical dimension of the area source
L	Length of the area source
W	Width of the area source
δ	Angle measured clockwise between north and the long side of the area source

A.2 PLUME-RISE FORMULAS

The effective stack height H of a buoyant plume is given by the sum of the physical stack height h and the buoyant rise Δh. For an adiabatic or unstable atmosphere, the buoyant rise Δh_N is given by

$$\Delta h_N = \left[\frac{1}{\bar{u}\{h\}} \left(\frac{3F}{2\gamma_1^2} \right)^{1/3} (10h)^{2/3} \right] f \qquad \text{(A-1)}$$

where the expression in the brackets is from Briggs (1971; 1972) and

$\bar{u}\{h\}$ = the mean wind speed at the stack height h

γ_1 = the adiabatic entrainment coefficient ~ 0.6

F = the initial buoyancy flux

$$= \frac{gV}{\pi} \left(1 - \frac{T_a}{T_s} \right) \qquad \text{(A-2)}$$

V = the volumetric emission rate of the stack

$$= \pi r^2 w$$

r = inner radius of stack

w = stack exit velocity

g = the acceleration due to gravity

T_a = the ambient air temperature (^oK)

T_s = the stack exit temperature (^oK)

The factor f, which limits the plume rise as the mean wind speed at stack height approaches or exceeds the stack exit velocity, is defined by

$$f = \begin{cases} 1 & ; \quad \bar{u}\{h\} \leq w/1.5 \\ \left(\frac{3w - 3\bar{u}\{h\}}{w}\right) & ; \quad w/1.5 < \bar{u}\{h\} < w \\ 0 & ; \quad \bar{u}\{h\} \geq w \end{cases} \qquad \text{(A-3)}$$

The empirical correction factor f is generally not applied to stacks with Froude numbers less than about unity. The corresponding Briggs (1971) rise formula for a stable atmosphere (potential temperature gradient greater than zero) is

$$\Delta h_S = \left\{ \begin{array}{ll} \left[\frac{6F}{\bar{u}\{h\}\ \gamma_2^{\,2}\ S}\right]^{1/3} & ; \ \pi\ \bar{u}\{h\}\ S^{-1/2} < 10h \\ \left[\frac{3F}{\bar{u}\{h\}\ \gamma_2^{\,2}\ S}\left(1 - \cos\left(\frac{10S^{1/2}\ h}{\bar{u}\{h\}}\right)\right)\right]^{1/3} & ; \ \pi\ \bar{u}\{h\}\ S^{-1/2} \geq 10h \end{array} \right\} f \qquad \text{(A-4)}$$

where

γ_2 = the stable entrainment coefficient ~ 0.66

$S = \frac{g}{T_a}\ \frac{\partial\theta}{\partial z}$

$\frac{\partial\theta}{\partial z}$ = vertical potential temperature gradient

The entrainment coefficients γ_1 and γ_2 are based on the suggestions of Briggs (1972). It should be noted that Equation (A-4) does not permit the calculated stable rise Δh_s to exceed the adiabatic rise Δh_N as the atmosphere approaches a neutral stratification ($\partial\theta/\partial z$ approaches 0). A procedure of this type is recommended by Briggs (1972).

A.3 SHORT-TERM CONCENTRATION MODEL

A.3.1 Elevated Sources

The atmospheric dispersion model used to calculate hourly average ground-level concentrations downwind from an elevated continuous source is given by

$$\chi\{x,y\} = \frac{K\,Q}{\pi\,\bar{u}\{H\}\,\sigma_y\,\sigma_z}\,\{\text{Vertical Term}\}\,\{\text{Lateral Term}\}\,\{\text{Decay Term}\} \qquad \text{(A-5)}$$

where

K = scaling coefficient to convert input parameters to dimensionally consistent units

Q = source emission rate

$\bar{u}\{H\}$ = mean wind speed at the plume stabilization height H

σ_y, σ_z = standard deviations of the lateral and vertical concentration distributions at downwind distance x

The Vertical Term refers to the plume expansion in the vertical or z direction and includes a multiple reflection term that limits cloud growth to the surface mixing layer.

$$\{\text{Vertical Term}\} = \left\{ \exp\left[-\frac{1}{2}\left(\frac{H}{\sigma_z}\right)^2\right] + \sum_{n=1}^{\infty}\left[\exp\left[-\frac{1}{2}\left(\frac{2n\,H_m + H}{\sigma_z}\right)^2\right] + \exp\left[-\frac{1}{2}\left(\frac{2n\,H_m - H}{\sigma_z}\right)^2\right]\right]\right\} \qquad \text{(A-6)}$$

where H_m is the depth of the surface mixing layer. The exponential terms in the infinite series in Equation (A-6) rapidly approach zero near the source. At the downwind distance where the exponential terms are non-zero for n equal 3, the plume has become approximately uniformly mixed within the surface mixing layer. In order to shorten computer computation time, Equation (A-6) is changed to the form

$$\{\text{Vertical Term}\} = \frac{\sqrt{2\pi}\,\sigma_z}{2H_m} \qquad \text{(A-7)}$$

beyond this point. Equation (A-7) changes the form of the vertical concentration distribution from Gaussian to rectangular. If H exceeds H_m, the vertical term is set equal to zero which results in a zero value for the ground-level concentration.

The Lateral Term refers to the crosswind expansion of the plume and is given by the expression

$$\{\text{Lateral Term}\} = \exp\left[-\frac{1}{2}\left(\frac{y}{\sigma_y}\right)^2\right] \qquad \text{(A-8)}$$

where y is the crosswind distance from the plume centerline to the point at which concentration is calculated.

The Decay Term, which accounts for the possibility of pollutant removal by physical or chemical processes, is of the form

$$\{\text{Decay Term}\} = \exp\left[-\psi\, x/\bar{u}\{H\}\right] \qquad \text{(A-9)}$$

where

ψ = the washout coefficient Λ (sec^{-1}) for precipitation scavenging

$= \frac{0.692}{T_{1/2}}$, where $T_{1/2}$ is the pollutant half life for physical or chemical removal

= 0 for no depletion (ψ is automatically set to zero by the computer program unless otherwise specified)

In the model calculations, the observed mean wind speed $\bar{u}_R$ is adjusted from the measurement height z_R to the source height h for plume-rise calculations and to the stabilization height H for the concentration calculations by a wind-profile exponent law

$$\bar{u}\{z\} = \bar{u}\{z_R\}\left(\frac{z}{z_R}\right)^p \qquad \text{(A-10)}$$

The exponent p, which is assigned on the basis of atmospheric stability, ranges from about 0.1 for very unstable conditions to about 0.4 for very stable conditions.

According to the derivation in the report by Cramer, et al. (1972), the standard deviation of the lateral concentration distribution σ_y is given by the expression

$$\sigma_y\{x\} = \sigma'_A x_{ry}\left[\frac{x + x_y - x_{ry}(1-\alpha)}{\alpha x_{ry}}\right]^{\alpha} \qquad \text{(A-11)}$$

$$x_y = \begin{cases} \dfrac{\sigma_{yR}}{\sigma'_A} - x_R & ; \ \dfrac{\sigma_{yR}}{\sigma'_A} \le x_{ry} \\ \alpha x_{ry}\left(\dfrac{\sigma_{yR}}{x_{ry}\,\sigma'_A}\right)^{1/\alpha} - x_R + x_{ry}(1-\alpha) & ; \ \dfrac{\sigma_{yR}}{\sigma'_A} > x_{ry} \end{cases} \qquad \text{(A-12)}$$

where

σ'_A = the standard deviation of the wind-azimuth angle in radians

x_{ry} = distance over which rectilinear plume expansion occurs downwind from an ideal point source (~ 50 meters)

σ_{yR} = the standard deviation of the lateral concentration distribution at downwind distance x_R

α = the lateral diffusion coefficient (~ 0.9)

The virtual distance x_y is not permitted to be less than zero. The lateral turbulent intensity σ'_A may be specified directly or may be assigned on the basis of the Pasquill stability category.

Following the derivation of Cramer, et al. (1972) and setting the vertical diffusion coefficient β equal to unity, the standard deviation of the vertical concentration distribution σ_z is given by the expression

$$\sigma_z\{x\} = \sigma'_E\left(x + x_z\right) \tag{A-13}$$

$$x_z = \left\{ \begin{array}{ll} \dfrac{\sigma_{zR}}{\sigma'_E} - x_R & ; \quad \dfrac{\sigma_{zR}}{\sigma'_E} \geq x_R \\ 0 & ; \quad \dfrac{\sigma_{zR}}{\sigma'_E} < x_R \end{array} \right\} \tag{A-14}$$

where

σ'_E = standard deviation of the wind-elevation angle in radians

σ_{zR} = the standard deviation of the vertical concentration distribution at downwind distance x_R

The vertical turbulent intensity σ'_E may also be obtained from direct measurements or may be assigned according to the Pasquill stability categories. When σ'_E values corresponding to the Pasquill stability categories are entered in Equation (A-13), the resulting curves will differ from the corresponding Pasquill-Gifford curves in that Equation (A-13) assumes rectilinear expansion at all downwind distances. Thus, σ_z values obtained from Equation (A-13) will be smaller than the values obtained from the Pasquill-Gifford A and B curves and larger than the values obtained from the D, E and F curves at long downwind distances. However, the multiple reflection term in Equation (A-6) which confines the plume to the surface mixing layer accounts for the behavior of the D, E and F curves (decrease in the expansion rate with distance) in a manner that may be related to the meteorology of the area.

Following the recommendations of Briggs (1972), the lateral and vertical standard deviations of a stabilized buoyant plume are defined by

$$\sigma_{yR} = \sigma_{zR} = \frac{0.5\,\Delta h}{2.15} \qquad \text{(A-15)}$$

The downwind distance to stabilization x_R is given by

$$x_R = \begin{cases} 10h & ; \quad \frac{\partial \theta}{\partial z} \leq 0 \\ \pi\, \bar{u}\{h\}\, S^{-1/2} & ; \quad \frac{\partial \theta}{\partial z} > 0 \text{ and } \pi\, \bar{u}\{h\}\, S^{-1/2} < 10h \\ 10h & ; \quad \frac{\partial \theta}{\partial z} > 0 \text{ and } \pi\, \bar{u}\{h\}\, S^{-1/2} \geq 10h \end{cases} \qquad \text{(A-16)}$$

A.3.2 Application of the Short-Term Model to Low-Level Emissions

The short-term diffusion model in Section A.3.1 may be used to calculate ground-level concentrations resulting from low-level emissions such as losses through building vents. These emissions are rapidly distributed by the cavity circulation of the building wake and quickly assume the dimensions of the building. Ground-level concentrations are calculated by setting the buoyancy parameter F equal to zero. The standard deviation of the lateral concentration distribution at the source σ_{yo} is defined by the building crosswind dimension y_o divided by 4.3. The standard deviation of the vertical concentration distribution at the source σ_{zo} is obtained by dividing the building height by 2.15. The initial dimensions σ_{yo} and σ_{zo} are assumed to be applicable at the downwind edge of the building. These procedures are in good agreement with the results of recent wind-tunnel experiments reported by Huber and Snyder (1976). It should be noted that separate turbulent intensities σ'_A and σ'_E may be defined for the low-level sources to account for the effects of surface roughness elements and heat sources.

A.3.3 Short-Term Concentration Model for Area Sources

The atmospheric dispersion model used to calculate ground-level concentrations at downwind distance x from the downwind edge of an area source is given by the expression

$$\chi\{x > x_o, y\} = \frac{K\,Q}{\sqrt{2\pi}\,\bar{u}\{h\}\,\sigma_z\{x\}\,y_o} \{\text{Vertical Term}\}$$

$$\{\text{Lateral Term}\}\ \{\text{Decay Term}\} \qquad \text{(A-17)}$$

where

Q = area source strength in units of mass per unit time

y_o = crosswind source dimension

$$\sigma_z\{x\} = \left\{ \begin{array}{ll} \dfrac{\sigma'_E\, x_o}{\ln\left[\dfrac{\sigma'_E(x+x_o)+h}{\sigma'_E(x)+h}\right]} & ; \quad x < 3x_o \\ \\ \sigma'_E(x+x_o/2)+h & ; \quad x \geq 3x_o \end{array} \right\} \qquad \text{(A-18)}$$

x_o = alongwind dimension of the area source

h = the characteristic height of the area source

The Vertical Term for an area source is given by

$$\{\text{Vertical Term}\} = \left\{ \begin{array}{ll} 1+2\sum_{n=1}^{3}\left\{\exp\left[-\frac{1}{2}\left(\frac{2n\,H_m}{\sigma_z\{x\}}\right)^2\right]\right\} & ; \exp\left[-\frac{1}{2}\left(\frac{6H_m}{\sigma_z}\right)^2\right] = 0 \\ \\ \dfrac{\sqrt{2\pi}\,\sigma_z\{x\}}{2\,H_m} & ; \exp\left[-\frac{1}{2}\left(\frac{6H_m}{\sigma_z}\right)^2\right] > 0 \end{array} \right\} \qquad \text{(A-19)}$$

The Lateral Term is given by the expression

$$\{\text{Lateral Term}\} = \left\{\text{erf}\left[\frac{y_o/2 + y}{\sqrt{2}\;\sigma_y\{x\}}\right] + \text{erf}\left[\frac{y_o/2 - y}{\sqrt{2}\;\sigma_y\{x\}}\right]\right\} \qquad \text{(A-20)}$$

where

y_o = crosswind dimension of the area source

y = crosswind distance from the centerline of the area source

and

$$\sigma_y\{x\} = \sigma'_A\left(x + x_o/2\right) \qquad \text{(A-21)}$$

The Decay Term is given by Equation (A-9) above.

The concentration at points interior to the area source is given by

$$\chi\{x'\} = \frac{2\,K\,Q}{\sqrt{2\pi}\,\bar{u}\{h\}\,x_o\,y_o\,\sigma'_E}\left\{\ln\left[\frac{\sigma'_E(x'+1)+h}{\sigma'_E+h}\right]\right\}\{\text{Vertical Term}\} \qquad \text{(A-22)}$$

where

x' = distance downwind from the upwind edge of the area source

A.4 LONG-TERM CONCENTRATION MODEL

A.4.1 Elevated Sources

The atmospheric dispersion model for elevated point and volume sources is similar in form to the Air Quality Display Model (Environmental Protection Agency, 1969) and the Climatological Dispersion Model (Calder, 1971). In the model, the area surrounding a continuous source of pollutants is divided into sectors of equal angular width corresponding to the class intervals of the seasonal and annual frequency distributions of wind direction. The emission rate during a season or year is partitioned according to the relative wind-direction frequencies. Ground-level concentration fields for each source are translated to a common reference coordinate grid system and summed to obtain the total due to all emissions. For a single source, the mean seasonal concentration at a point (r, θ) is given by

$$\chi_{\ell}\{r,\theta\} = \frac{2KQ}{\sqrt{2\pi}\, r\, \Delta\theta'} \sum_{i,j,k} \left[\frac{f_{i,j,k,\ell}}{\bar{u}_i \{H_{i,k,\ell}\}\, \sigma_{z;i,k,\ell}} \; S\{\theta\} \; V_{i,k,\ell} \right. \tag{A-23}$$

$$\left. \exp\left[-\psi\, r/\bar{u}_i \{H_{i,k,\ell}\} \right] \right]$$

$$V_{i,k,\ell} = \exp\left[-\frac{1}{2}\left(\frac{H_{i,k,\ell}}{\sigma_{z;i,k,\ell}} \right)^2 \right] + \sum_{n=1}^{\infty} \left\{ \exp\left[-\frac{1}{2}\left(\frac{2n\, H_{m;i,k,\ell} - H_{i,k,\ell}}{\sigma_{z;i,k,\ell}} \right)^2 \right] \right. \tag{A-24}$$

$$\left. + \exp\left[-\frac{1}{2}\left(\frac{2n\, H_{m;i,k,\ell} + H_{i,k,\ell}}{\sigma_{z;i,k,\ell}} \right)^2 \right] \right\}$$

where

$f_{i,j,k,\ell}$ = frequency of occurrence of the i^{th} wind-speed category, j^{th} wind-direction category and k^{th} stability or time-of-day category for the ℓ^{th} season

$\Delta\theta'$ = the sector width in radians

$S\{\theta\}$ = a smoothing function

$$S\{\theta\} = \left\{ \begin{array}{ll} \dfrac{\Delta\theta' - \left|\theta'_j - \theta'\right|}{\Delta\theta'} & ; \quad \left|\theta'_j - \theta'\right| \leq \Delta\theta' \\ 0 & ; \quad \left|\theta'_j - \theta'\right| > \Delta\theta' \end{array} \right\} \tag{A-25}$$

θ'_j = the angle measured in radians from north to the centerline of the j^{th} wind-direction sector

θ' = the angle measured in radians from north to the point (r, θ)

As with the short-term model, the Vertical Term given by Equation (A-24) is changed to the form

$$V_{i,k,\ell} = \frac{\sqrt{2\pi}\ \sigma_{z;i,k,\ell}}{2H_{m;i,k,\ell}} \qquad \text{(A-26)}$$

when the exponential terms in Equation (A-24) become non-zero for n equal 3. The remaining terms in Equations (A-23) and (A-24) are identical to those previously defined in Section A.3.1 for the short-term model, except that the turbulent intensities and potential temperature gradients may be separately assigned to each wind-speed and/or stability (or time-of-day) category; the ambient air temperatures may be separately assigned to each stability (or time-of-day) category for each season; and the surface mixing depths may be separately assigned to each wind-speed and/or stability (or time-of-day) category for each season.

As shown by Equation (A-25), the rectangular concentration distribution within a given angular sector is modified by the function $S\{\theta\}$ which smoothes discontinuities in the concentration at the boundaries of adjacent sectors. The centerline concentration in each sector is unaffected by contributions from adjacent sectors. At points off the sector centerline, the concentration is a weighted function of the concentration at the centerline of the sector in which the calculation is being made and the concentration at the centerline of the nearest adjoining sector.

The mean annual concentration at the point (r, θ) is calculated from the seasonal concentrations using the expression

$$\chi_a\{r,\theta\} = \frac{1}{4}\sum_{\rho}\chi_{\rho}\{r,\theta\} \qquad \text{(A-27)}$$

A.4.2 Application of the Long-Term Model to Low-Level Emissions

Long-term ground-level concentrations produced by low-level emissions are calculated from Equation (A-23) by setting the buoyancy parameter F equal to zero. The standard deviation of the vertical concentration distribution at the downwind edge of the building σ_{zo} is defined as the building height divided by 2.15. Separate vertical turbulent intensities σ_E^1 may be defined for the low-level sources to account for the effects of surface heat sources and roughness elements. A virtual point source is used to account for the initial lateral dimension of the source in a manner identical to that described below for area sources.

A.4.3 Long-Term Concentration Model for Area Sources

The mean seasonal concentration at downwind distance r with respect to the center of an area source is given by the expression

$$\chi_\ell\{r > r_o\} = \frac{2KQ}{\sqrt{2\pi}\, R\, \Delta\theta'} \left\{ \sum_{i,j,k} \left[\frac{f_{i,j,k,\ell}}{\bar{u}_i\{h\}\, \sigma_{z;i,k}} \; S\{\theta\} \; V_{i,k,\ell} \right] \right.$$

$$\left. \exp\left[-\psi(r' - r_o)/\bar{u}_i\{h\} \right] \right\} \qquad \text{(A-28)}$$

where

R = radial distance from the virtual point source to the receptor

$$= \left((r' + x_y)^2 + y^2 \right)^{1/2}$$

r' = distance from source center to receptor, measured along the plume axis

r_o = effective source radius

y = lateral distance from the cloud axis to the receptor

x_y = virtual distance

$$= r_o \cot \frac{\Delta\theta'}{2} \tag{A-29}$$

$$\sigma_{z;i,k} = \left\{ \begin{array}{ll} \dfrac{2\sigma'_{E;i,k}\, r_o}{\ln\left[\dfrac{\sigma'_{E;i,k}(r'+r_o)+h}{\sigma'_{E;i,k}(r'-r_o)+h}\right]} & ; \quad r_o < r' < 6r_o \\ \\ \sigma'_{E;i,k}\, r'+h & ; \quad r' \geq 6r_o \end{array} \right\} \tag{A-30}$$

$$V_{i,k,\ell} = \left\{ \begin{array}{ll} 1+2\displaystyle\sum_{n=1}^{3} \exp\left[-\frac{1}{2}\left(\frac{2n\,H_{m;i,k,\ell}}{\sigma_{z;i,k}}\right)^2\right] & ; \exp\left[-\frac{1}{2}\left(\frac{6H_{m;i,k,\ell}}{\sigma_{z;i,k}}\right)^2\right] = 0 \\ \\ \dfrac{\sqrt{2\pi}\ \sigma_{z;i,k}}{2H_{m;i,k,\ell}} & ; \exp\left[-\frac{1}{2}\left(\frac{6H_{m;i,k,\ell}}{\sigma_{z;i,k}}\right)^2\right] > 0 \end{array} \right\} \tag{A-31}$$

and the remaining parameters are identical to those previously defined.

For points interior to the area source, the concentration for seasonal models is given by the expression

$$\chi_\ell\{r \leq r_o\} = \frac{2KQ}{\sqrt{2\pi}\ x_o\ y_o} \sum_{i,j,k} \left[\frac{f_{i,j,k,\ell}}{\bar{u}_i\{h\}\ \sigma'_{E;i,k}} \ln\left[\frac{\sigma'_{E;i,k}(r''+1)+h}{\sigma'_{E;i,k}+h}\right] V_{i,k,\ell}\right] \tag{A-32}$$

where

r'' = the downwind distance, measured along the plume axis from the upwind edge of the area source

A.5 APPLICATION OF THE SHORT-TERM AND LONG-TERM CONCENTRATION MODELS IN COMPLEX TERRAIN

The short-term and long-term concentration models described in Sections A.3 and A.4 are strictly applicable only for flat terrain where the base of the stack (or the building source) and the ground surface downwind from the source are at the same elevation. However, both models may also be applied to complex terrain by defining effective stabilization heights and mixing depths. The following assumptions are made in the model calculations for complex terrain:

- The top of the surface mixing layer extends over the calculation grid at a constant height above mean sea level
- Ground-level concentrations at all grid points above the top of the surface mixing layer are zero
- Plumes that stabilize above the top of the surface mixing layer do not contribute to ground-level concentrations at any grid point (this assumption also applies to flat terrain)

In order to determine whether the stabilized plume is contained within the surface mixing layer, it is necessary to calculate the mixing depth $H_m^*\{z_s\}$ at the source from the relationship

$$H_m^*\{z_s\} = \left(H_m + z_a - z_s\right) \qquad \text{(A-33)}$$

where

H_m = the depth of the surface mixing layer measured at a point with elevation z_a above mean sea level

z_s = the height above mean sea level of the source

Equation (A-33) is represented schematically in Figure A-1. As shown by the figure, the actual top of the surface mixing layer is assumed to remain at a constant elevation above mean sea level. If the height H of the stabilized plume above the base of the stack is less than or equal to $H_m^*\{z_s\}$, the plume is defined to be contained within the surface mixing layer.

The height H_o of the stabilized plume above mean sea level is given by the sum of the height H of the stabilized plume above the base of the stack and the elevation z_s of the base of the stack. At any elevation z above mean sea level, the effective height $H'\{z\}$ of the plume centerline above the terrain is then given by

$$H'\{z\} = \begin{cases} H_o - z & ; \quad H_o - z \geq 0 \\ 0 & ; \quad H_o - z < 0 \end{cases} \qquad \text{(A-34)}$$

The effective mixing depth $H_m'\{z\}$ above a point at elevation z above mean sea level is defined by

$$H_m'\{z\} = \begin{cases} H_m & ; \quad z \geq z_a \\ H_m + z_a - z & ; \quad z < z_a \end{cases} \qquad \text{(A-35)}$$

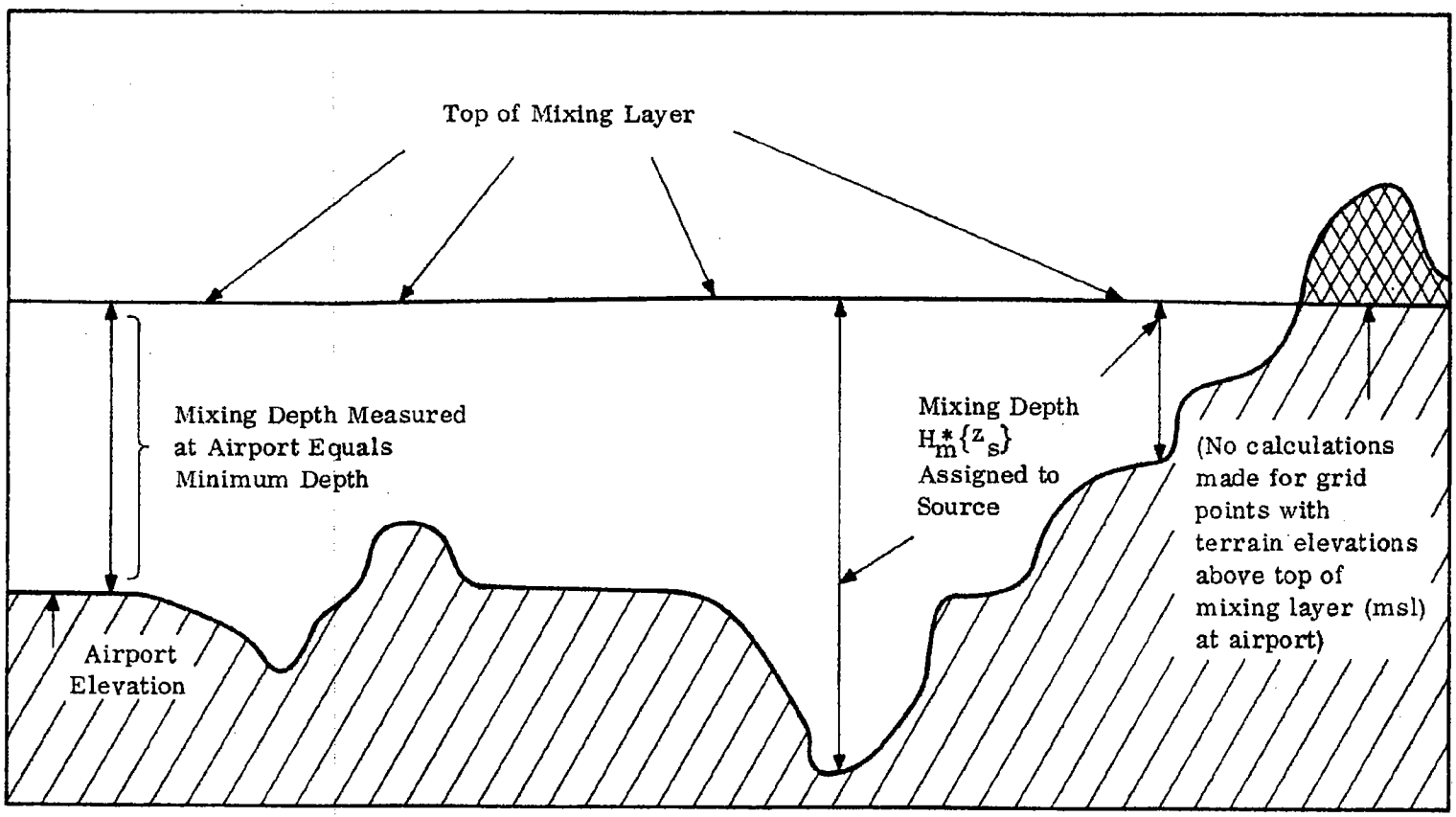

FIGURE A-1. Mixing depth $H_m^*\{z_s\}$ used to determine whether the stabilized plume is contained within the surface mixing layer.

Figure A-2 illustrates the assumptions implicit in Equation (A-35). For grid points at elevations below the airport elevation, the effective mixing depth $H_m'\{z\}$ is allowed to increase in a manner consistent with Figure A-1. However, in order to prevent a physically unrealistic compression of plumes as they pass over elevated terrain, the effective mixing depth is not permitted to be less than the mixing depth measured at the airport. It should be noted that the concentration is set equal to zero for grid points above the actual top of the mixing layer (see Figure A-1).

The terrain adjustment procedures also assume that the mean wind speed at any given height above sea level is constant. Thus, the wind speed $\bar{u}_R$ measured at height z_R above the surface at a point with elevation z_a above mean sea level is adjusted to the stack height for the plume-rise calculations by the relationship

$$\bar{u}\{h\} = \left\{ \begin{array}{ll} \bar{u}_R \left(\dfrac{h_o - z_a}{z_R} \right)^p & ; \quad h_o \geq z_a + z_R \\ \\ \bar{u}_R & ; \quad h_o < z_a + z_R \end{array} \right\} \qquad \text{(A-36)}$$

where h_o is the height above mean sea level of the top of the stack. Similarly, the wind speed $\bar{u}\{H\}$ used in the concentration calculations is given by

$$\bar{u}\{H\} = \left\{ \begin{array}{ll} \bar{u}_R \left(\dfrac{H_o - z_a}{z_R} \right)^p & ; \quad H_o \geq z_a + z_R \\ \\ \bar{u}_R & ; \quad H_o < z_a + z_R \end{array} \right\} \qquad \text{(A-37)}$$

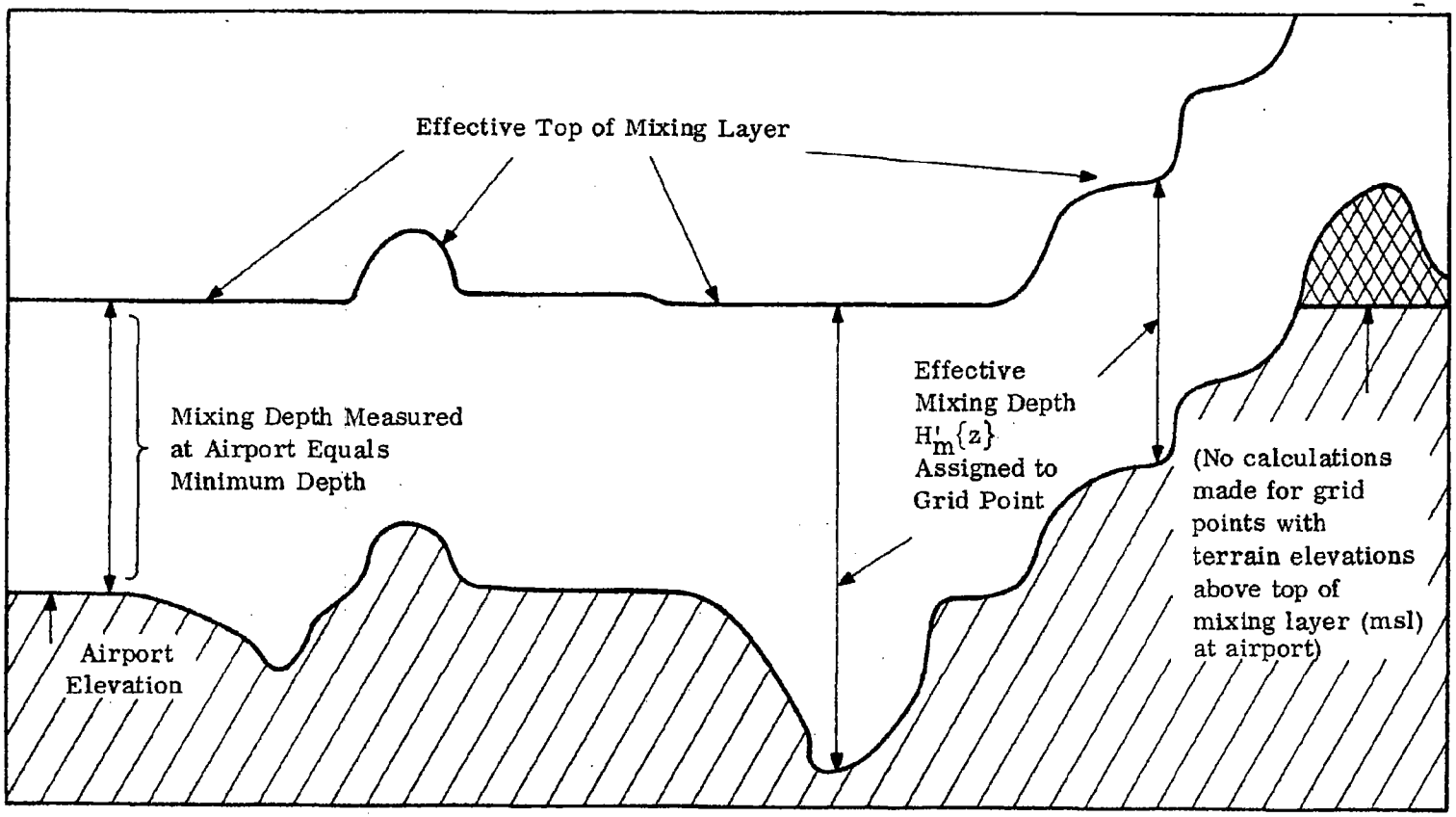

FIGURE A-2. Effective mixing depth $H'_m\{z\}$ assigned to grid points for the concentration calculations.

It should be noted that the terrain-adjustment procedures outlined above provide a very simple representation of complex plume-terrain interactions that are not yet well understood. Because the model assumptions are generally conservative, it is possible that concentrations calculated for elevated terrain, especially elevated terrain near a source, exceed the concentrations that actually occur. It should also be noted that the procedures described above differ from previous "terrain-intersection" models in that terrain intersection is only permitted for a plume contained within a mixing layer. That is, terrain intersection is permitted for all stability categories, but only for a plume contained within the surface mixing layer.

APPENDIX B

SUPPLEMENTARY METEOROLOGICAL DATA

Table B-1 lists the dates and hours of the "worst-case" 3-hour and 24-hour periods for any point, for the Deep Creek Mountains potential Class I region and for the City of Tooele. The hourly meteorological inputs for these periods are listed in chronological order in Tables B-2 through B-7. The procedures used to develop the hourly meteorological inputs given in Tables B-2 through B-7 are discussed in Section 2.3.3.

TABLE B-1

DATES AND HOURS OF "WORST-CASE" 3-HOUR
AND 24-HOUR PERIODS

Area	Dates and Hours (MST)	
	3-Hour	24-Hour
Any Point (Vicinity of the Plant)	1-2 December 1951 2200-0000	22-23 June 1950 2200-2100
Deep Creek Mountains	13 November 1954 0200-0400	1-2 November 1953 0900-0800
City of Tooele	31 October 1952 0800-1000	30-31 October 1950 0700-0600

TABLE B-2

HOURLY METEOROLOGICAL INPUTS FOR THE PERIOD 2200 MST
ON 22 JUNE 1950 TO 2100 MST ON 23 JUNE 1950

Hour (MST)	Wind Direction (deg)	Wind Speed (m/sec)	Mixing Depth (m)	Ambient Air Temperature (°K)	Potential Temperature Gradient (°K/m)	Wind-Profile Exponent	Vertical Turbulent Intensity (rad)	Lateral Turbulent Intensity (rad)
2200	203	11.84	2400	296	0.000	0.10	0.0465	0.1111
2300	203	11.33	2400	295	0.000	0.10	0.0465	0.1111
2400	203	9.78	2250	295	0.000	0.10	0.0465	0.1111
0100	203	6.18	1950	294	0.000	0.10	0.0465	0.1111
0200	203	8.75	2250	294	0.000	0.10	0.0465	0.1111
0300	203	14.41	2400	294	0.000	0.10	0.0465	0.1111
0400	203	11.84	2400	293	0.000	0.10	0.0465	0.1111
0500	203	12.36	2400	293	0.000	0.10	0.0465	0.1111
0600	203	13.38	2400	293	0.000	0.10	0.0465	0.1111
0700	203	15.44	2400	295	0.000	0.10	0.0465	0.1111
0800	203	14.93	2400	296	0.000	0.10	0.0465	0.1111
0900	203	14.41	2400	299	0.000	0.10	0.0465	0.1111
1000	203	15.44	2400	299	0.000	0.10	0.0465	0.1111
1100	203	14.93	4000	300	0.000	0.10	0.0735	0.1310
1200	203	16.47	4000	301	0.000	0.10	0.0735	0.1310
1300	203	16.99	4000	302	0.000	0.10	0.0735	0.1310

TABLE B-2 (Continued)

Hour (MST)	Wind Direction (deg)	Wind Speed (m/sec)	Mixing Depth (m)	Ambient Air Temperature (^{o}K)	Potential Temperature Gradient (^{o}K/m)	Wind-Profile Exponent	Vertical Turbulent Intensity (rad)	Lateral Turbulent Intensity (rad)
1400	225	14.93	4000	303	0.000	0.10	0.0465	0.1009
1500	225	12.36	2400	303	0.000	0.10	0.0465	0.1009
1600	225	12.36	2400	303	0.000	0.10	0.0465	0.1009
1700	203	13.38	2400	302	0.000	0.10	0.0465	0.1009
1800	203	15.96	2400	301	0.000	0.10	0.0465	0.1009
1900	203	15.44	2400	299	0.000	0.10	0.0465	0.1009
2000	203	10.81	2250	296	0.000	0.10	0.0465	0.1009
2100	180	8.24	1950	295	0.000	0.10	0.0465	0.1009

TABLE B-3

HOURLY METEOROLOGICAL INPUTS FOR THE PERIOD 0700 MST ON 30 OCTOBER 1950 TO 0600 MST ON 31 OCTOBER 1950

Hour (MST)	Wind Direction (deg)	Wind Speed (m/sec)	Mixing Depth (m)	Ambient Air Temperature (^{o}K)	Potential Temperature Gradient (^{o}K/m)	Wind-Profile Exponent	Vertical Turbulent Intensity (rad)	Lateral Turbulent Intensity (rad)
0700	193	4.6	860	287	0.005	0.15	0.0465	0.0665
0800	180	1.0	800	288	0.000	0.20	0.0735	0.1051
0900	193	4.6	1600	291	0.000	0.10	0.0735	0.1051
1000	193	8.2	1125	293	0.000	0.10	0.0465	0.1223
1100	193	12.4	1625	295	0.000	0.10	0.0465	0.1223
1200	193	14.4	1625	296	0.000	0.10	0.0465	0.1223
1300	193	11.8	1625	297	0.000	0.10	0.0465	0.1223
1400	193	13.4	1625	297	0.000	0.10	0.0465	0.1223
1500	193	14.4	1625	297	0.000	0.10	0.0465	0.1223
1600	193	14.4	1625	295	0.000	0.10	0.0465	0.1223
1700	193	11.3	1625	293	0.000	0.10	0.0465	0.1223
1800	193	11.3	1625	292	0.000	0.10	0.0465	0.1223
1900	193	9.3	1275	291	0.000	0.10	0.0465	0.1223
2000	193	5.7	1125	290	0.000	0.10	0.0465	0.1223
2100	193	5.7	1125	288	0.000	0.10	0.0465	0.1223
2200	193	5.7	1125	288	0.000	0.10	0.0465	0.1223

TABLE B-3 (Continued)

Hour (MST)	Wind Direction (deg)	Wind Speed (m/sec)	Mixing Depth (m)	Ambient Air Temperature (^{o}K)	Potential Temperature Gradient (^{o}K/m)	Wind-Profile Exponent	Vertical Turbulent Intensity (rad)	Lateral Turbulent Intensity (rad)
2300	193	7.7	1125	288	0.000	0.10	0.0465	0.1223
0000	193	7.2	1125	288	0.000	0.10	0.0465	0.1223
0100	193	8.2	1125	288	0.000	0.10	0.0465	0.1223
0200	193	7.7	1125	287	0.000	0.10	0.0465	0.1223
0300	193	9.3	1275	288	0.000	0.10	0.0465	0.1223
0400	193	7.2	1125	286	0.000	0.10	0.0465	0.1223
0500	193	6.7	1125	285	0.000	0.10	0.0465	0.1223
0600	193	8.2	1125	286	0.000	0.10	0.0465	0.1223

TABLE B-4

HOURLY METEOROLOGICAL INPUTS FOR THE PERIOD 2200 MST ON 1 DECEMBER 1951 TO 0000 MST ON 20 DECEMBER 1951

Hour (MST)	Wind Direction (deg)	Wind Speed (m/sec)	Mixing Depth (m)	Ambient Air Temperature (^{o}K)	Potential Temperature Gradient (^{o}K/m)	Wind-Profile Exponent	Vertical Turbulent Intensity (rad)	Lateral Turbulent Intensity (rad)
2200	203	4.12	460	277	0.005	0.15	0.0465	0.0829
2300	203	4.12	460	279	0.005	0.15	0.0465	0.0829
0000	203	4.63	460	277	0.005	0.15	0.0465	0.0829

TABLE B-5

HOURLY METEOROLOGICAL INPUTS FOR THE PERIOD 0800 TO 1000 MST
ON 31 OCTOBER 1952

Hour (MST)	Wind Direction (deg)	Wind Speed (m/sec)	Mixing Depth (m)	Ambient Air Temperature (^{o}K)	Potential Temperature Gradient (^{o}K/m)	Wind-Profile Exponent	Vertical Turbulent Intensity (rad)	Lateral Turbulent Intensity (rad)
0800	193	3.1	860	279	0.005	0.15	0.0465	0.0829
0900	193	5.1	860	284	0.005	0.15	0.0465	0.0829
1000	193	5.1	860	290	0.005	0.15	0.0465	0.0829

TABLE B-6

HOURLY METEOROLOGICAL INPUTS FOR THE PERIOD 0900 TO 0800 MST
ON 1-2 NOVEMBER 1953

Hour (MST)	Wind Direction (deg)	Wind Speed (m/sec)	Mixing Depth (m)	Ambient Air Temperature (^{o}K)	Potential Temperature Gradient (^{o}K/m)	Wind-Profile Exponent	Vertical Turbulent Intensity (rad)	Lateral Turbulent Intensity (rad)
0900	124	3.1	860	280	0.005	0.15	0.0465	0.0829
1000	124	2.1	690	283	0.010	0.20	0.0465	0.0829
1100	124	2.6	690	286	0.010	0.20	0.0465	0.0829
1200	124	4.1	1600	288	0.000	0.10	0.0735	0.1051
1300	180	3.6	1600	289	0.000	0.10	0.0735	0.1051
1400	202	5.1	860	291	0.005	0.15	0.0465	0.0665
1500	225	3.1	690	292	0.005	0.15	0.0465	0.0665
1600	Calm		800	291	0.000	0.20	0.0735	0.1051
1700	Calm		125	288	0.040	0.30	0.0235	0.0336
1800	180	3.6	860	286	0.005	0.15	0.0465	0.0665
1900	180	3.6	125	284	0.010	0.20	0.0350	0.0501
2000	157	3.6	125	285	0.010	0.20	0.0350	0.0501
2100	180	3.1	125	285	0.010	0.20	0.0350	0.0531
2200	180	2.6	125	283	0.020	0.25	0.0350	0.0531
2300	180	3.1	125	284	0.010	0.20	0.0350	0.0531
0000	124	3.6	860	284	0.005	0.15	0.0465	0.0665

TABLE B-6 (Continued)

Hour (MST)	Wind Direction (deg)	Wind Speed (m/sec)	Mixing Depth (m)	Ambient Air Temperature (^{o}K)	Potential Temperature Gradient (^{o}K/m)	Wind-Profile Exponent	Vertical Turbulent Intensity (rad)	Lateral Turbulent Intensity (rad)
0100	157	4.1	860	285	0.005	0.15	0.0465	0.0665
0200	124	4.6	860	285	0.005	0.15	0.0465	0.0665
0300	157	3.6	860	285	0.005	0.15	0.0465	0.0665
0400	124	2.6	125	284	0.020	0.25	0.0350	0.0501
0500	157	2.6	125	284	0.020	0.25	0.0350	0.0501
0600	124	3.6	860	284	0.005	0.15	0.0465	0.0665
0700	157	2.6	125	284	0.020	0.25	0.0350	0.0501
0800	180	3.6	860	288	0.005	0.15	0.0465	0.0665

TABLE B-7

HOURLY METEOROLOGICAL INPUTS FOR THE PERIOD 0200 TO 0400 MST
ON 13 NOVEMBER 1954

Hour (MST)	Wind Direction (deg)	Wind Speed (m/sec)	Mixing Depth (m)	Ambient Air Temperature (^{o}K)	Potential Temperature Gradient (^{o}K/m)	Wind-Profile Exponent	Vertical Turbulent Intensity (rad)	Lateral Turbulent Intensity (rad)
0200	124	3.6	860	277	0.005	0.15	0.0465	0.0829
0300	124	2.1	690	276	0.010	0.20	0.0465	0.0829
0400	124	1.5	460	276	0.020	0.25	0.0465	0.0829